Journal of Applied Mathematics in Science and Technology

Volume No. 13

Issue No. 1

January - April 2025

ENRICHED PUBLICATIONS PVT.LTD

JE - 18,Gupta Colony, Khirki Extn,
Malviya Nagar, New Delhi - 110017.
E- Mail: info@enrichedpublication.com
Phone :- +91-8877340707

Journal of Applied Mathematics in Science and Technology

Aims and Scope

The Journal of Applied Mathematics in Science and Technology is published quarterly by Enriched publications. Journal of Applied Mathematics in Science and Technology is peer reviewed journal and monitored by a team of reputed editorial board members. This journal consists of research articles, reviews, and case studies on Science Technology. This journal mainly focuses on the latest and most common subjects of its domain.

Journal of Applied Mathematics in Science and Technology

Journal of Applied Mathematics in Science and Technology

(Volume No. 13, Issue No. 1, Jan - Apr 2025)

Contents

Normal ordering of degenerate integral powers of number operator and its applications

Taekyun Kima,DaeSanKimb andHyeKyungKimc
aDepartment of Mathematics, Kwangwoon University, Seoul, Republic of Korea;
bDepartment of Mathematics, Sogang University, Seoul, Republic of Korea;
cDepartment of Mathematics Education, Daegu Catholic University, Gyeonsang, Republic of Korea

ABSTRACT

The normal ordering of an integral power of the number operator in terms of boson operators is expressed with the help of the Stirling numbersofthesecondkind.Asa'degenerateversion'ofthis,we consider the normal ordering of a degenerate integral power of the number operator in terms of boson operators, which is represented by means of the degenerate Stirling numbers of the second kind. As an application of this normal ordering, we derive two equations defining the degenerate Stirling numbers of the second kind and a Dobinski-like formula for the degenerate Bell polynomials.

KEYWORDS Normal ordering; coherent states; degenerate Stirling numbers ofthe second kind; degenerate Bell numbers

1. Introduction

The Stirling number of the second S2(n,k) is the number of ways to partition a set of n objects into k nonempty subsets. The Stirling numbers of the second kind have been extensively studied and repeatedly and independently rediscovered during their long history. The Stirling numbers of the second kind appear in many different contexts and have numerous applications, for example to enumerative combinatorics and quantum mechanics. They are given either by (5) or by (7). The study of degenerate versions of some special numbers and polynomials began with Carlitz's paper in [1], where the degenerate BernoulliandEulernumberswereinvestigated.Itisremarkablethatinrecentyearsquite a few degenerate versions of special numbers and polynomials have been explored with diverse tools and yielded many interesting results (see [2–4] and the references therein). It turns out that the degenerate Stirling numbers of the second play an important role in this exploration for degenerate versions of many special numbers and polynomials. The normal ordering of an integral power of the number operator a†a in terms of boson operators a and a† can bewritten in the form

$$(a^{\dagger}a)^{k} = \sum_{l=0}^{k} S_2(k,l)(a^{\dagger})^{l}a^{l}.$$

In addition, the normal ordering of the degenerate kth power of the number operator a†a, namely (a†a)k,λ, in terms of boson operators a and a† can be written in the form

$$(a^{\dagger}a)_{k,\lambda} = \sum_{l=0}^{k} S_{2,\lambda}(k,l)(a^{\dagger})^{l}a^{l}, \tag{1}$$

where the generalized falling factorials (x)n,λ are given by (3) and the degenerate Stirling numbers S2,λ(k,l) by (4) and (6).

Theaimofthispaperistousethenormalorderingin(1)inordertoderivetwoequations defining the degenerate Stirling numbers of the second kind (see (4), (6)) and a Dobinskilike formula for the degenerate Bell numbers (see (37)). In more detail, our main results are as follows. Firstly, by applying the degenerate kth power (a†a)k,λ to any number states |m, m=0,1,2,... and using (1) we obtain Equation (4). Secondly, by comparing one expression of z|ea†a λ (t)|z obtained by using (1) and another one of it obtained by solving a differential equation we get Equation (6). Thirdly, we obtain a Dobinski-like fromula for the degenerate Bell numbers φk,λ by showing that z|(a†a)k,λ|z is equal to φk,λ(|z|2) by using (1) and that it is also equal to some other expression coming from the representation of coherent state in terms of number states. For the rest of this section, we recall what are needed throughout this paper.

For any λ ∈ R,thedegenerate exponential functions are defined by

$$e_{\lambda}^{x}(t) = \sum_{k=0}^{\infty} \frac{(x)_{n,\lambda}}{k!}t^{k}, \quad (\text{see } [1-4]), \tag{2}$$

where the generalized falling factorials $(x)_{n,\lambda}$ are defined by

$$(x)_{0,\lambda} = 1, \quad (x)_{n,\lambda} = x(x-\lambda)\cdots\big(x-(n-1)\lambda\big), \quad (n \geq 1). \tag{3}$$

When $x = 1$, we let $e_{\lambda}(t) = e_{\lambda}^{1}(t) = \sum_{k=0}^{\infty} \frac{(1)_{k,\lambda}}{k!}t^{k}$. The degenerate Stirling numbers of the second kind are defined by

$$(x)_{n,\lambda} = \sum_{k=0}^{n} S_{2,\lambda}(n,k)(x)_{k}, \quad (n \geq 0), \quad (\text{see } [2,5,6]), \tag{4}$$

where $(x)_0 = 1$, $(x)_n = x(x-1)\cdots(x-n+1)$, $(n \geq 1)$.

Note that $\lim_{\lambda\to 0} S_{2,\lambda}(n,k) = S_2(n,k)$ are the ordinary Stirling numbers of the second kind given by

$$x^{n} = \sum_{k=0}^{n} S_2(n,k)(x)_{k}, \quad (n \geq 0), \quad (\text{see } [2,7,8]). \tag{5}$$

From (4), we note that

$$\frac{1}{k!}\big(e_\lambda(t)-1\big)^k=\sum_{n=k}^{\infty}S_{2,\lambda}(n,k)\frac{t^n}{n!},\quad (k\geq 0),\quad \text{(see [2])}. \tag{6}$$

By letting $\lambda\to 0$ in (6), we see that the Stirling numbers of the second kind are also given by

$$\frac{1}{k!}\big(e^t-1\big)^k=\sum_{n=k}^{\infty}S_2(n,k)\frac{t^n}{n!},\quad (k\geq 0),\quad \text{(see [2, 9])}. \tag{7}$$

In [4], the degenerate Bell polynomials are defined by

$$e^{x(e_\lambda(t)-1)}=\sum_{n=0}^{\infty}\phi_{n,\lambda}(x)\frac{t^n}{n!}. \tag{8}$$

Thus, by (8), we get

$$\phi_{n,\lambda}(x)=\sum_{k=0}^{n}S_{2,\lambda}(n,k)x^k,\quad (n\geq 0),\quad \text{(see [3, 4, 10])}.$$

When $x=1$, $\phi_{n,\lambda}=\phi_{n,\lambda}(1)$ are called the degenerate Bell numbers.

From (4), we note that

$$S_{2,\lambda}(n+1,k)=S_{2,\lambda}(n,k-1)+(k-n\lambda)S_{2,\lambda}(n,k),\quad \text{(see [2])}, \tag{9}$$

where $n,k\in\mathbb{N}$ with $n\geq k$.

In this paper, we pay attention to some properties with the boson operators a and $a^\dagger$ that satisfy

$$[a,a^\dagger]=aa^\dagger-a^\dagger a=1,\quad \text{(see [11, 12])}.$$

The normal ordering of an integral power of the number operator $a^\dagger a$ in terms of boson operators a and $a^\dagger$ can be written in the form

$$(a^\dagger a)^k=\sum_{l=0}^{k}S_2(k,l)(a^\dagger)^l a^l,\quad \text{(see [11, 12])}. \tag{10}$$

The number states $|m\rangle$, $m = 0, 1, 2, \ldots$, are defined as

$$a|m\rangle = \sqrt{m}|m-1\rangle, \quad a^\dagger|m\rangle = \sqrt{m+1}|m+1\rangle. \tag{11}$$

By (11), we get $a^\dagger a|m\rangle = m|m\rangle$. The coherent states $|z\rangle$, where z is a complex number, satisfy $a|z\rangle = z|z\rangle$, $\langle z|z\rangle = 1$. To show a connection to coherent states, we recall that the harmonic oscillator has Hamiltonian $H = a^\dagger a$ (neglecting the zero point energy) and the usual eigenstates $|n\rangle$ (for $n \in \mathbb{N}$) satisfying $H|n\rangle = n|n\rangle$ and $\langle m|n\rangle = \delta_{m,n}$, where $\delta_{m,n}$ is Kronecker's symbol.

2. Normal ordering of degenerate integral powers of the number operator and its applications.

First, we recall the definition of coherent states $a|z\rangle = z|z\rangle$, equivalently $\langle z|a^\dagger = \langle z|\overline{z}$, where $z \in \mathbb{C}$. For the coherent states $|z\rangle$, we write

$$|z\rangle = \sum_{n=0}^{\infty} A_n|n\rangle. \tag{12}$$

Then, by (12), we get

$$a|z\rangle = \sum_{n=0}^{\infty} A_n a|n\rangle = \sum_{n=1}^{\infty} A_n\sqrt{n}|n-1\rangle, \tag{13}$$

and

$$a|z\rangle = z|z\rangle = z\sum_{n=0}^{\infty} A_n|n\rangle = \sum_{n=1}^{\infty} zA_{n-1}|n-1\rangle. \tag{14}$$

From (13) and (14), we have

$$A_n = \frac{z}{\sqrt{n}}A_{n-1} = \frac{z}{\sqrt{n}}\frac{z}{\sqrt{n-1}}A_{n-2} = \cdots = \frac{z^n}{\sqrt{n!}}A_0. \tag{15}$$

So, by (12) and (15), we get

$$|z\rangle = A_0\sum_{n=0}^{\infty}\frac{z^n}{\sqrt{n!}}|n\rangle. \tag{16}$$

By the property of coherent state $|z\rangle$, we get

$$\begin{aligned} 1 = \langle z|z\rangle &= \overline{A}_0\sum_{m=0}^{\infty}\frac{\overline{z}^m}{\sqrt{m!}}A_0\sum_{n=0}^{\infty}\frac{z^n}{\sqrt{n!}}\langle m|n\rangle \\ &= |A_0|^2\sum_{n=0}^{\infty}\frac{|z|^{2n}}{n!} = |A_0|^2 e^{|z|^2}. \end{aligned} \tag{17}$$

Thus, by (17), we get

$$A_0 = e^{-\frac{1}{2}|z|^2} e^{i(\text{arbitrary phase})}.$$

Discarding the phase factors, by (16), we get

$$|z\rangle = e^{-\frac{|z|^2}{2}} \sum_{n=0}^{\infty} \frac{z^n}{\sqrt{n!}} |n\rangle. \tag{18}$$

For $x, y \in \mathbb{C}$, we have

$$\begin{aligned}\langle x|y\rangle &= e^{-\frac{|x|^2}{2}} \sum_{m=0}^{\infty} \frac{(\overline{x})^m}{\sqrt{m!}} e^{-\frac{|y|^2}{2}} \sum_{n=0}^{\infty} \frac{y^n}{\sqrt{n!}} \langle m|n\rangle \\ &= e^{-\frac{|x|^2}{2}-\frac{|y|^2}{2}} \sum_{n=0}^{\infty} \frac{(\overline{x}y)^n}{n!} = e^{-\frac{1}{2}(|x|^2+|y|^2)+\overline{x}y}.\end{aligned}$$

We recall that the standard bosonic commutation relation $[a, a^\dagger] = aa^\dagger - a^\dagger a = 1$ can be considered formally, in a suitable space of functions f, by letting $a = \frac{\mathrm{d}}{\mathrm{d}x}$ and $a^\dagger = x$ (the operator of multiplication by x). From (3), we note that

$$\left(x\frac{\mathrm{d}}{\mathrm{d}x}\right)_{n,\lambda} f(x) = \sum_{k=1}^{n} S_{2,\lambda}(n,k) x^k \left(\frac{\mathrm{d}}{\mathrm{d}x}\right)^k f(x), \tag{19}$$

where n is a positive integer.

Now, we consider the normal ordering of a degenerate integral power of the number operator $a^\dagger a$ in terms of the boson operators a and $a^\dagger$. In view of (19), the normal ordering of the degenerate kth power of the number operator $a^\dagger a$ in terms of boson operators a and $a^\dagger$ can be written in the form

$$(a^\dagger a)_{k,\lambda} = \sum_{l=0}^{k} S_{2,\lambda}(k,l)(a^\dagger)^l a^l, \quad (k \in \mathbb{N}). \tag{20}$$

From (11) and (20), we note that

$$(a^\dagger a)_{k,\lambda}|m\rangle = (a^\dagger a)(a^\dagger a - \lambda)\cdots(a^\dagger a - (k-1)\lambda|m\rangle = (m)_{k,\lambda}|m\rangle, \tag{21}$$

and

$$(a^\dagger a)_{k,\lambda}|m\rangle = \sum_{l=0}^{k} S_{2,\lambda}(k,l)(a^\dagger)^l a^l|m\rangle = \sum_{l=0}^{k} S_{2,\lambda}(k,l)(m)_l|m\rangle. \tag{22}$$

Thus, by (21) and (22), we get

$$(m)_{k,\lambda} = \sum_{l=0}^{k} S_{2,\lambda}(k,l)(m)_l, \quad (k \geq 1). \tag{23}$$

Equation (29) can be rewritten as

$$f(t) = e^{|z|^2(e_\lambda(t)-1)} = \sum_{l=0}^{\infty} |z|^{2l} \frac{1}{l!}(e_\lambda(t)-1)^l. \tag{30}$$

From (25), we note that

$$f(t) = \sum_{k=0}^{\infty} \frac{t^k}{k!} \left(\sum_{l=0}^{k} S_{2,\lambda}(k,l)|z|^{2l} \right) = \sum_{l=0}^{\infty} \left(\sum_{k=l}^{\infty} S_{2,\lambda}(k,l) \frac{t^k}{k!} \right) |z|^{2l}. \tag{31}$$

Therefore, by (30) and (31), we get

$$\frac{1}{l!}\big(e_\lambda(t)-1\big)^l = \sum_{k=l}^{\infty} S_{2,\lambda}(k,l)\frac{t^k}{k!},$$

which agrees with (6). From (24), we have

$$\langle z|(a^\dagger a)_{k,\lambda}|z\rangle = \sum_{l=0}^{k} S_{2,\lambda}(k,l)|z|^{2l} = \phi_{k,\lambda}(|z|^2). \tag{32}$$

Setting $|z| = 1$, we obtain

$$\langle z|(a^\dagger a)_{k,\lambda}|z\rangle = \phi_{k,\lambda}, \quad (k \geq 1). \tag{)}$$

Differentiating (25) with respect to t, we obtain

$$\begin{aligned} \frac{\partial f(t)}{\partial t} &= \sum_{k=1}^{\infty} \frac{t^{k-1}}{(k-1)!}\phi_{k,\lambda}(|z|^2) = \sum_{k=0}^{\infty} \phi_{k+1,\lambda}(|z|^2)\frac{t^k}{k!}. \\ &= \langle z|a^\dagger e_\lambda^{a^\dagger a+1-\lambda}(t)a|z\rangle = e_\lambda^{1-\lambda}(t)\langle z|a^\dagger e_\lambda^{a^\dagger a}(t)a|z\rangle \end{aligned} \tag{33}$$

On the other hand, by (28), we get

$$\begin{aligned} \frac{\partial f(t)}{\partial t} &= e_\lambda^{1-\lambda}(t)|z|^2 f(t) = e_\lambda^{1-\lambda}(t)|z|^2 \sum_{k=0}^{\infty} \frac{t^k}{k!}\phi_{k,\lambda}(|z|^2) \\ &= |z|^2 \sum_{k=0}^{\infty} \left(\sum_{l=0}^{k} \binom{k}{l} (1-\lambda)_{k-l,\lambda}\phi_{l,\lambda}(|z|^2) \right) \frac{t^k}{k!}. \end{aligned} \tag{34}$$

Thus, by (33) and (34), we get

$$\phi_{k+1,\lambda}(|z|^2) = |z|^2 \sum_{l=0}^{k} \binom{k}{l} (1-\lambda)_{k-l,\lambda}\phi_{l,\lambda}(|z|^2).$$

In particular, for $|z| = 1$, we have

$$\phi_{k+1,\lambda} = \sum_{l=0}^{k} \binom{k}{l} (1-\lambda)_{k-l,\lambda} \phi_{l,\lambda}.$$

Evaluating the left hand side of (32) by using the representation of the coherent state in terms of the number state in (18), we have

$$\begin{aligned} \langle z|(a^{\dagger}a)_{k,\lambda}|z\rangle &= e^{-\frac{|z|^2}{2}} \cdot e^{-\frac{|z|^2}{2}} \sum_{m,n=0}^{\infty} \frac{\bar{z}^m z^n}{\sqrt{m!}\sqrt{n!}} (n)_{k,\lambda} \langle m|n\rangle \\ &= e^{-|z|^2} \sum_{n=0}^{\infty} \frac{|z|^{2n}}{n!} (n)_{k,\lambda}. \end{aligned} \tag{35}$$

Thus, by (32) and (35), we get

$$\begin{aligned} \phi_{k,\lambda}(|z|^2) &= \sum_{l=0}^{k} |z|^{2l} S_{2,\lambda}(k,l) = e^{-|z|^2} \sum_{n=0}^{\infty} \frac{|z|^{2n}}{n!} (n)_{k,\lambda} \\ &= e^{-|z|^2} \sum_{n=1}^{\infty} \frac{|z|^{2n}}{(n-1)!} (n-\lambda)_{k-1,\lambda}, \quad (k \in \mathbb{N}). \end{aligned} \tag{36}$$

In particular, by letting $|z| = 1$, we get

$$\phi_{k,\lambda} = \frac{1}{e} \sum_{n=0}^{\infty} \frac{1}{n!} (n)_{k,\lambda} = \frac{1}{e} \sum_{n=1}^{\infty} \frac{1}{(n-1)!} (n-\lambda)_{k-1,\lambda}, \quad (k \in \mathbb{N}). \tag{37}$$

This is a Dobinski-like formula for the degenerate Bell numbers.

3. Conclusion

Intensive studies have been done for degenerate versions of quite a few special polynomials and numbers by using such tools as combinatorial methods, generating functions, mathematical physics, umbral calculus techniques, p-adic analysis, differential equations, special functions, probability theory and analytic number theory.

As a degenerate version of the well-known normal ordering of an integral power of the number operator, we considered the normal ordering of a degenerate integral power of the number operator in terms of boson operators. By using this normal ordering we derived two equations defining the degenerate Stirling numbers of the second kind and a Dobinski-like formula for the degenerate Bell numbers.

It is one of our future projects to continue to explore various degenerate versions of many special polynomials and numbers by using aforementioned tools.

Acknowledgements

Theauthorswouldliketothankthereviewersfortheirhelpfulcommentsandsuggestions.

Disclosure statement

Nopotential conflict of interest was reported by the author(s).

Funding

This workwassupportedbytheBasicScienceResearchProgram,theNationalResearchFoundation of Korea, (NRF-2021R1F1A1050151).

References

[1] Carlitz L. Degenerate Stirling, Bernoulli and Eulerian numbers. Utilitas Math. 1979;15:51–88.

[2] Kim DS, Kim T. A note on a new type of degenerate Bernoulli numbers. Russ J Math Phys. 2020;27(2):227–235.

[3] Kim T, Kim DS. On some degenerate differential and degenerate difference operator. Russ J Math Phys. 2022;29(1):37–46.

[4] Kim T, Kim DS, Dolgy DV. On partially degenerate Bell numbers and polynomials. Proc Jangjeon Math Soc. 2017;20(3):337–345.

[5] KimT,KimDS,JangL-C,etal.Representations of degenerate Hermite polynomials. Adv Appl Math. 2022;139:Paper No. 102359.

[6] Kim T, Kim DS. Some identities on truncated polynomials associated with degenerate Bell polynomials. Russ J Math Phys. 2021;28(3):342–355.

[7] AraciS.AnewclassofBernoullipolynomialsattachedtopolyexponentialfunctionsandrelated identities. Adv Stud Contemp Math (Kyungshang). 2021;31(2):195–204.

[8] Jang L, Kim DS, Kim H, et al. Study of degenerate poly-Bernoulli polynomials by λ-umbral calculus. CMES Comput Model Eng Sci. 2021;129(1):393–408.

[9] KimT,KimDS,KimHK,etal.SomepropertiesondegenerateFubinipolynomials.ApplMath Sci Eng. 2022;30(1):235–248.

[10] Kim T, Kim DS, Lee H, et al. New properties on degenerate Bell polynomials. Complexity. 2021;2021:Article ID 7648994, 12 pages.

[11] Katriel J. Bell numbers and coherent states. Phys Lett A. 2000;273(3):159–161.

[12] Perelomov A. Generalized coherent states and their applications. Texts and Monographs in Physics. Berlin: Springer-Verlag; 1986. p. xii+320.

Groundwater flow in karstic aquifer: analytic solution of dual-porosity fractional model to simulate groundwater flow

Mahaveer Prasad Yadav, Ritu Agarwal, Sunil Dutt Purohit, Devendra Kumar & Daya Lal Suthar

aDepartment of Mathematics, Amity University Rajasthan, Jaipur, Rajasthan, India; bDepartment of Mathematics, Malaviya National Institute of Technology, Jaipur, India; cDepartment of HEAS (Mathematics), Rajasthan Technical University, Kota, India; dDepartment of Mathematics, University of Rajasthan, Jaipur, Rajasthan, India; eDepartment of Mathematics, Wollo University, Dessie, Ethiopia

ABSTRACT

Karst aquifers have a very complex flow system because of their high spatial heterogeneity of void distribution. In this manuscript, flow simulation has been used to investigate the flow mechanism in a fissured karst aquifer with double porosity, revealing how to connect exchange and storage coefficients to the volumetric density of the highly permeable form of media. The governing space-time differential equations of the dual-porosity model are modified by using the Caputo–Fabrizio fractional derivative operator for time memory. The sensitivity of exchange and storage coefficients has been demonstrated using numerical studies with theoretical karst systems in this hybrid system. When dealing with highly heterogeneous systems, it is demonstrated that porosity storage and exchange coefficients are required. The analytical model could possibly reveal some of the karstic network's essential structural features.

KEYWORDS Karstaquifer; dual-porosity model; Caputo–Fabrizio fractional operator; Laplace transform

1. Introduction

An aquifer is a geological structure of rocks, fractured rocks and sands, that occur at different levels in groundwater and can store and transmit the groundwater. Karst aquifers are a particular category of broken rock aquifer (calcareous, dolomite or magnesite) in which comparatively fragile rock are dissolved by the water in the cracks, greatly expanding the size of the fractures. These solution cavities can be tens of metres broad in some areas, and form underground cave systems. In karst aquifers, groundwater flow is more intense and higher than in other types of aquifers.

In general, the fissured karstic aquifers are schematized into an unknown high permeability channel network associated with low permeability fractured limestone to a discharge field. The structure of channel network has an important role in hydraulic reaction in such carbonate aquifers, assimilated to the dual porosity model, but a priori is never well

understood[1,2]. Karstic aquifer with adual-porosity systemhasdividedintoporositysystems, one is primary porosity which has low permeability (matrix volume) and secondary porosity which has high permeability channel network (karstic network). In the hydraulic channel, these two components are then associated with duality. In the literature, Cornaton et al. [3] derived one-dimensional analytical porosityweighted solutions of the dual-porosity model using the integral transform technique, and Warren et al. [4] developed an idealized model for the purpose of studying the characteristic behaviour of a permeable medium of naturally fractured or vugular reservoir and investigated unsteady-state flow in reservoir analytically. Kazemi [5]devisedanideal mathematical framework of a naturally fractured reservoir with a uniform fracture distribution, consisting of a finite circular reservoir with a centrally positioned well and two separateporoussectors,matrixandfracture,respectively.Steady-stateexchangemodelsare less complex than transient exchange models in view of mathematical or physical points. Moench [6] studied the pseudo steady-state block/fracture exchange model and showed that the hydraulic behaviour of aquifer lies in only a high permeability aquifer and doesn't require a low permeability aquifer (block).

Barenblatt et al. [7]definedthefluxexchangeasqef =±α(hm − hf),wherehm is the mean hydraulic head in matrix continua, hf is the average hydraulic head in fractured continua and α being the exchange coefficient which is related to fractured geometry [4]. The dual-porosity approach is a powerful technique to simulate groundwater flow in a fracturedaquifer.Langetal. [8] modelled dual-porosity approach for acoustic propagation through heterogeneous porous structures in the fractured aquifer. It consists of two continua, one is more permeable and the other is less permeable. Moutsopoulos et al. [9] obtained a numerical solution using dual-porosity approach, qualitative behaviour is also described.Prideetal.[10] constructed the governing equations of linear acoustics of composites comprising dual porous constituents isotropic in nature, using volume-averaging arguments. Agarwal et al. [11] examined the concept of miscible flow in porous media with longitudinal dispersion and evaluated the solution of governing differential equation employing the Caputo–Fabrizio fractional derivative operator that has a non-singular kernel.

Many authors have applied the fractional derivatives without singular kernels such as Atangana et al. [12] proposed a novel formulation of the idea of fractional-order derivatives, which heusedtocalculatetheflowofwaterinsidealeakingaquifer.In[13],Atangana established the properties of the Caputo–Fabrizio fractional derivative and used the valuable tools for solving the nonlinear Fisher's reaction-diffusion problem. Baleanu et al. [14] showed that four fractional integro-differential inclusions have solutions. Under certain conditions,thesetofsolutionsforthesecondfractionalintegro-differentialinclusionproblem is infinite dimensional. Atangana et al. [15] proposed a model of the subsurface water movement via aquifer and extended using an alternative definition of Caputo–Fabrizio

fractional derivative.

Yavuz et al. [16–18] proposed and investigated fractional order models described by a fractional operator and found analytical/numerical solutions to the constructed problems by using the Laplace transform method. Baleanu et al. [14,19,20]investigatedsome new class of hybrid type fractional differential equations and inclusions via some nonlocal three-point boundary value conditions and showed that the dimension of the set of solutions for the second fractional integro-differential inclusion problem is infinite dimensional under somedifferent conditions. Ageneralized fractional model is also introduced for the COVID-19 pandemic, including the effects of isolation and quarantine. Qureshi et al. [21] numerically approximated the Caputo–Fabrizio fractional derivative operatorusingthetwo-pointfinite forwarddifference formulaforfirst-orderordinary derivative of the function. Jajarmi et al. [20,22] investigated the complex behaviours of a capacitor microphone dynamical system and the asymptotic behaviour of immunogenic tumour dynamics based on a new fractional model constructed by the concept of general fractional operators. Thabet et al. [23] explored the existence and uniqueness criteria for a newcoupledCaputoconformablesystemofpantographproblems.Mataretal.[24]investigated the motion of abeamonaninternallybentnanowire byusingthe fractional calculus theory.

The solutions of two fractional models of Jeffrey's fluid modelled with Caputo and Caputo–Fabrizio fractional derivatives were compared by Ahmad et al. [25]. Aleem et al. [26] presented the unsteady MHD nanofluid flow travelling through an accelerating infinite vertical plate positioned in porous material involving the above two fractional operators. Asjad et al. [27] compared these two fractional differential operators for the time fractional unsteady flows of a second-grade fluid with Newtonian heating. Yang et al. [28] presented a new fractional derivative and used the Laplace transform to provide an analyticalsolutionforthefractional-orderheatflow. In[29], Yang et al. developed the first analytical solution of anomalous diffusion equations combining the general derivatives with the decayexponential kernel using the Laplace transform. In [30], Yang et al. used the Laplace transform to obtain series solutions for the generalized fractional-order diffusion equations. According to transient-type input boundary conditions, we give one-dimensional analytical solutions tothedual-porositymodelofthegoverningfractionaldifferentialequation in this study. In this system, we further discuss the relationship between the exchange coeff icient and specific geometrical and/or physical properties of the highly permeable zones. To determine the hydraulic responses of karstic aquifers, numerical models are used.

2. Mathematicalpreliminaries

The definition of the Caputo–Fabrizio fractional derivative operator [31]isgivenas

$$ {}_{a}^{CF}D_{t}^{\alpha} f(t) = \frac{M(\alpha)}{1-\alpha} \int_{a}^{t} f'(\tau) \exp\left(-\alpha \frac{t-\tau}{1-\alpha}\right) \mathrm{d}\tau, \quad a < t < b, \tag{1} $$

where $f \in H'(a,b)$, $b > a, 0 < \alpha \leq 1$ and $M(\alpha)$ is a normalized function defined as

$$ M(\alpha) = 1 - \alpha + \frac{\alpha}{\Gamma(\alpha)}, \tag{2} $$

s.t. $M(0) = M(1) = 1$.

Laplace transform of the Caputo–Fabrizio fractional derivative is given as [31]

$$ \mathcal{L}\left[{}_{0}^{CF}D_{t}^{\alpha} f(t); s\right] = M(\alpha) \frac{sF(s) - f(0)}{s + \alpha(1-s)}, \quad 0 < \alpha \leq 1, \tag{3} $$

if exists.

3. Flow in channel continua

In this section, we will derive the solution of one-dimensional governing differential equation using the dual-porosity approach. Here, the matrix conductivity has been assumed zero, and exchange kinetics between porosities has been assumed to be first order [3]. The governing differential equation for controlling flow in channel continua is given as

$$ K_c \frac{\partial^2 h_c(x,t)}{\partial x^2} = S_c \frac{\partial h_c(x,t)}{\partial t} + S_m \frac{\partial h_m(x,t)}{\partial t}, \tag{4} $$

where S_c and K_c are the storage coefficient and hydraulic conductivity in the high permeability channel continuum, respectively and S_m is the storage coefficient in the low permeability matrix continuum. The term $S_m \frac{\partial h_m(x,t)}{\partial t}$ acts as the source term.

In the channel continuum, volumetric density is $\theta = \frac{V_c}{V_a}$ and in the matrix continuum it is given as $1 - \theta = \frac{V_m}{V_a}$, where V_c is the volume of channel, V_m is the volume of matrix and V_a denotes the total volume. Now, weighting the terms of Equation (4) with θ and $1 - \theta$ gives

$$ \begin{aligned} \theta K_c \frac{\partial^2 h_c(x,t)}{\partial x^2} &= \theta S_c \frac{\partial h_c(x,t)}{\partial t} + (1-\theta) S_m \frac{\partial h_m(x,t)}{\partial t} \\ \implies K_c \frac{\partial^2 h_c(x,t)}{\partial x^2} &= S_c \frac{\partial h_c(x,t)}{\partial t} + \beta S_m \frac{\partial h_m(x,t)}{\partial t}, \end{aligned} \tag{5} $$

where

$$ \beta = \frac{1-\theta}{\theta}. \tag{6} $$

When continuum are assimilated into tubes or pipes, then Equation (6) becomes

$$\beta = \left(\frac{r_m}{r_c}\right)^2, \tag{7}$$

where r_c and r_m are the radius of channel and matrix respectively.

The obtained solution of Equation (5) must satisfy the following initial and boundary conditions:

$$h_c(0,t) = f(t), \tag{8}$$

$$h_c(x,0) = h_m(x,0) = 0, \tag{9}$$

$$h_c(\pm\infty,t) = 0, \tag{10}$$

$$-K_c\frac{\partial h_c(0,t)}{\partial x} = f(t), \tag{11}$$

where $f(t)$ is a transient input function.

From Equation (5), storage in matrix, by considering first-order transfer in porosities is given as

$$S_m\frac{\partial h_m(x,t)}{\partial t} = -\alpha(h_m - h_c). \tag{12}$$

Now, using the non-singular time-Caputo–Fabrizio fractional differential operator in Equations (5) and (12), respectively, we obtain

$$K_c\frac{\partial^2 h_c(x,t)}{\partial x^2} = S_c\frac{\partial^\eta h_c(x,t)}{\partial t^\eta} + \beta S_m\frac{\partial^\zeta h_m(x,t)}{\partial t^\zeta}, \tag{13}$$

$$S_m\frac{\partial^\zeta h_m(x,t)}{\partial t^\zeta} = -\alpha(h_m(x,t) - h_c(x,t)), \tag{14}$$

where $0 < \eta \leq 1, 0 < \zeta \leq 1, t > 0$ and $x \in \mathbb{R}^+$.

Applying the Laplace transform with respect to the time derivative on Equations (13) and (14) and setting the initial conditions mentioned in (9), we obtain

$$K_c\frac{d^2\bar{h}_c(x,p)}{\mathrm{d}x^2} = S_c\frac{p\bar{h}_c(x,p)}{p(1-\eta)+\eta} + \beta S_m\frac{p\bar{h}_m(x,p)}{p(1-\zeta)+\zeta} \tag{15}$$

$$S_m\frac{p\bar{h}_m(x,p)}{p(1-\zeta)+\zeta} = \alpha(\bar{h}_m(x,p) - \bar{h}_c(x,p)). \tag{16}$$

Further, by solving Equations (15) and (16), we obtain

$$\frac{\mathrm{d}^2\bar{h}_c(x,p)}{\mathrm{d}x^2} = M(p)\bar{h}_c(x,p), \tag{17}$$

Further, by solving Equations (15) and (16), we obtain

$$\frac{\mathrm{d}^2\bar{h}_c(x,p)}{\mathrm{d}x^2} = M(p)\bar{h}_c(x,p), \tag{17}$$

where

$$M(p) = \frac{1}{K_c}\left[S_c\frac{p}{p(1-\eta)+\eta} + \beta S_m\alpha\frac{p}{S_m p + \alpha p(1-\zeta)+\alpha\zeta}\right]. \tag{18}$$

The general solution of Equation (17) is obtained as

$$\bar{h}_c(x,p) = \frac{1}{2}\left([\bar{r}_1(p)+\bar{r}_2(p)]e^{x\sqrt{M(p)}} + [\bar{r}_2(p)-\bar{r}_1(p)]e^{-x\sqrt{M(p)}}\right), \tag{19}$$

where $\bar{r}_1(p)$ and $\bar{r}_2(p)$ are boundary conditions.

Now to satisfy the boundary condition (10), we have $\bar{r}_1(p) = -\bar{r}_2(p)$, and for the condition (8), $\bar{r}_2(p) = \bar{f}(p) = \mathcal{L}[f(t);p]$. Applying these results to Equation (19), we obtain

$$\bar{h}_c(x,p) = \bar{f}(p)e^{-x\sqrt{M(p)}}. \tag{20}$$

For the function $\bar{f}(p) = \mathcal{L}[\delta(t);p] = 1$, $\delta(t)$ being Dirac delta function. For the channel transfer function Equation (20) becomes

$$\bar{h}_c(x,p) = e^{-x\sqrt{M(p)}}, \tag{21}$$

and Darcy flux is given as

$$\bar{q}_c(x,p) = -K_c\frac{\mathrm{d}\bar{h}_c(x,p)}{\mathrm{d}x} = K_c\sqrt{M(p)}e^{-x\sqrt{M(p)}}, \tag{22}$$

and at $x = 0$

$$-K_c\frac{\mathrm{d}\bar{h}_c(x,p)}{\mathrm{d}x} = \mathcal{L}[\delta(t);p] = 1. \tag{23}$$

Now, in the channel, the transformed hydraulic head becomes

$$\bar{h}_c(x,p) = \frac{e^{-x\sqrt{M(p)}}}{K_c\sqrt{M(p)}}, \tag{24}$$

and hence the transformed flux is given by

$$\bar{q}_c(x,p) = e^{-x\sqrt{M(p)}}, \tag{25}$$

which is equal to the transfer defined in Equation (21).

One can obtain the inverse Laplace transform of Equation (20) by applying the convolution theorem as

$$h_c(x,t) = \int_0^t e^{-x\sqrt{M(t-\tau)}} f(\tau)\,\mathrm{d}\tau = \int_0^t G(t-\tau) f(\tau)\,\mathrm{d}\tau, \tag{26}$$

where

$$G(t) = \mathcal{L}^{-1}[e^{-x\sqrt{Mp}}; t], \tag{27}$$

is the Green function.

4. Relationship between channels using transfer function

We assume that

$$\mathrm{tr}(x,p) = e^{-x\sqrt{M(p)}}, \tag{28}$$

where $\mathrm{tr}(x,p)$ is the transfer function in the dual permeability approach. Using the flux boundary condition $-K_c \frac{\mathrm{d}\bar{h}_c(0,p)}{\mathrm{d}x} = f(p)$, solution of Equation (17) reads

$$\bar{h}_c(x,p) = \frac{f(p)}{K_c} \int_x^\infty \mathrm{tr}(u,p)\,\mathrm{d}u. \tag{29}$$

Transformed flux in the channel head is

$$\bar{q}_c(x,p) = f(p)\,\mathrm{tr}(x,p), \tag{30}$$

and

$$h_m = \frac{\alpha h_c}{\frac{S_m}{1-\zeta}\left(\frac{1}{t} - \frac{\zeta}{1-\zeta} e^{\frac{\zeta t}{1-\zeta}}\right) + \frac{\alpha}{t}}, \tag{31}$$

where h_m is hydraulic head in the matrix and the flow rate is given by

$$Q_c(x,t) = q_c(x,t)\pi r_c^2. \tag{32}$$

The flow model in Equation (29) and Equation (30) described the dual-porosity transfer function model.

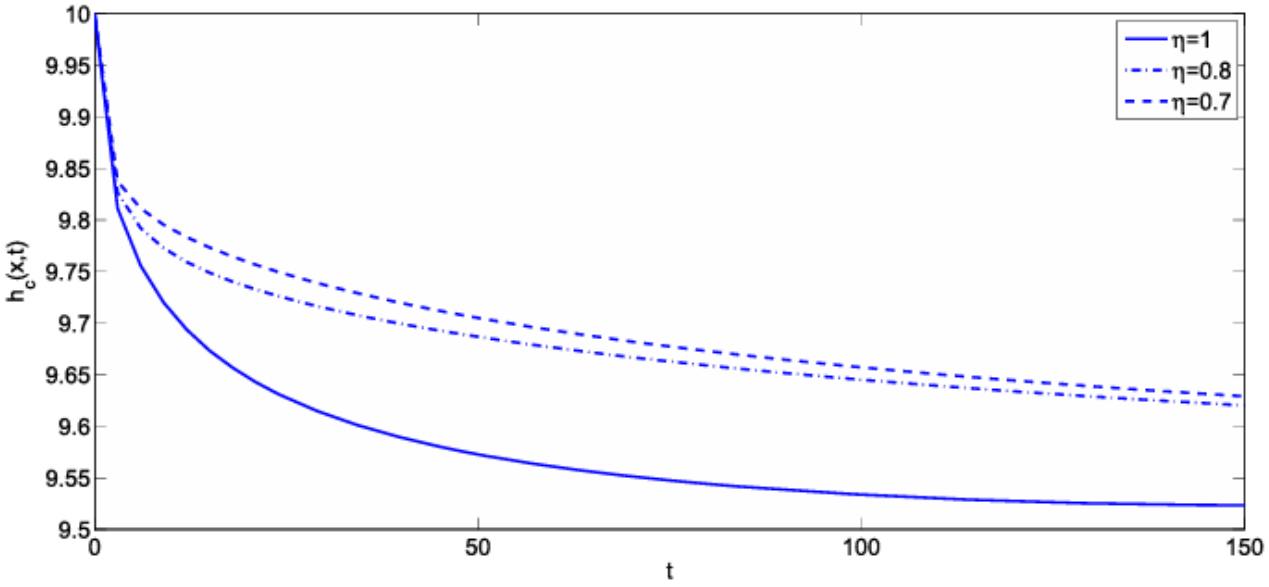

(a)

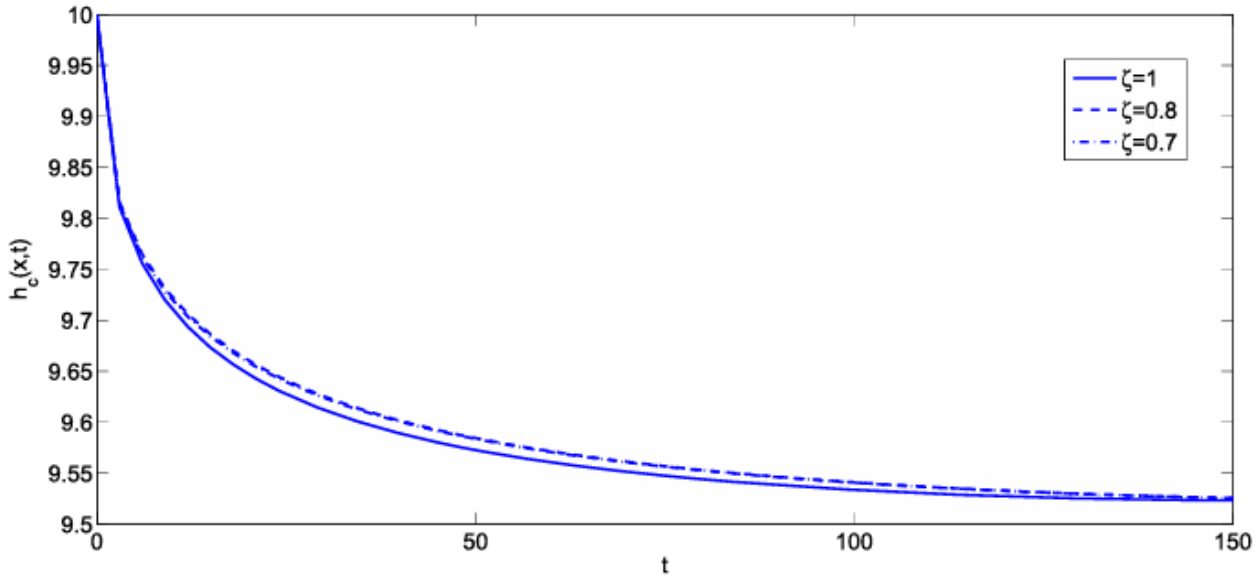

(b)

Figure 1. Simulated hydraulic head w.r.t. fixed coefficient $K_c = 10\,\mathrm{m}^3\,\mathrm{s}^{-1}$, $S_c = 5 \times 10^{-2}\,\mathrm{m}$, $S_m = 10^{-4}\,\mathrm{m}$, $\alpha = 10^{-3}$, $x = 150\,\mathrm{m}$ and in (a) for $\zeta = 1$, $\eta = 1, 0.8, 0.7$, in (b) for $\eta = 1$, $\zeta = 1, 0.8, 0.7$.

5. Numerical simulation

Let incremental volume in channel continua is $\pi r_c^2\,\mathrm{d}x$, then exchange flux q_{ef} can be formulated as [3]

$$q_{ef} = -\alpha[h_m - h_c]\frac{r_c}{2}, \tag{33}$$

and using Darcy's law q_{ef} yields

$$q_{ef} = -K_m \frac{h_m - h_c}{\epsilon r_m}, \tag{34}$$

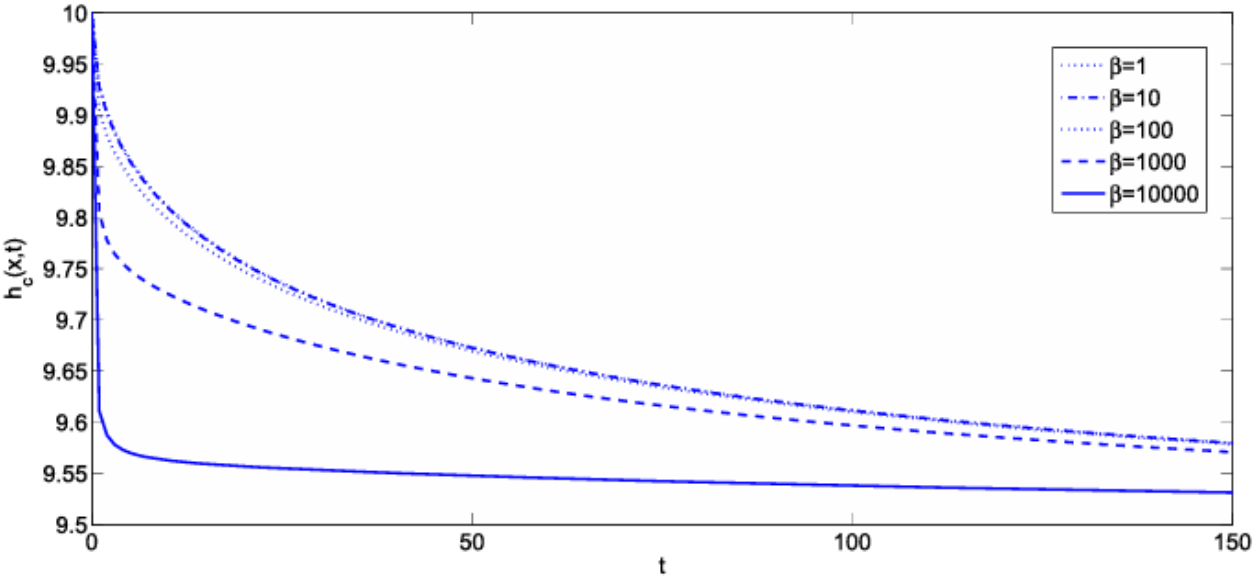

(a)

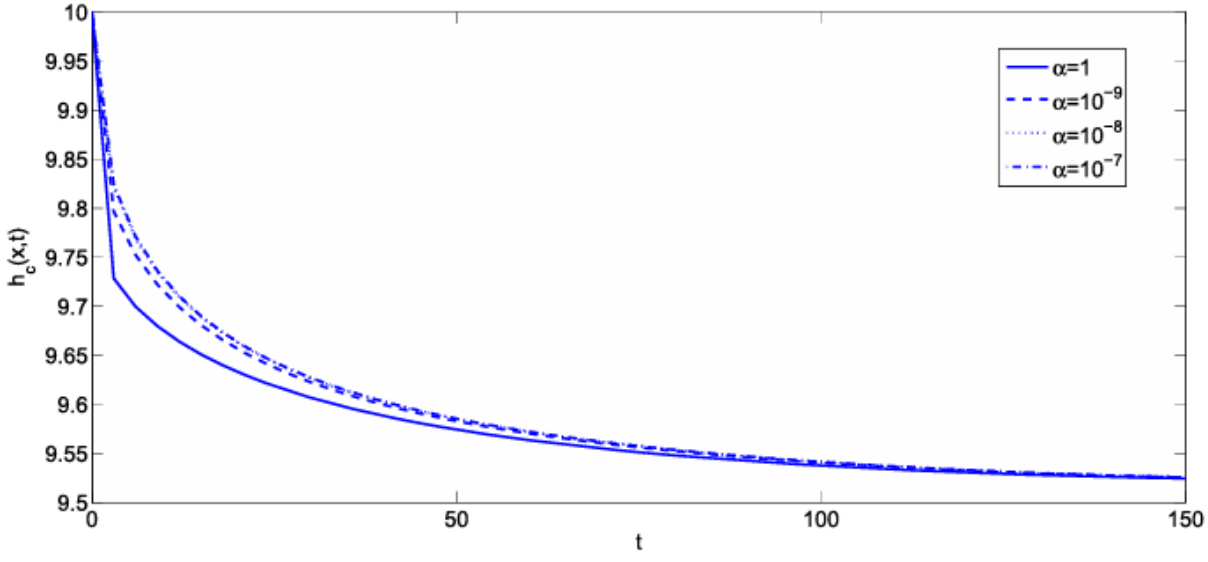

(b)

Figure 2. Simulated hydraulic head w.r.t. fixed coefficient $K_c = 10\,\mathrm{m}^3\,\mathrm{s}^{-1}, S_c = 5 \times 10^{-2}\,\mathrm{m}, S_m = 10^{-4}\,\mathrm{m}, x = 150\,\mathrm{m}, \eta = 1, \zeta = 1$ and in (a) for fixed $\alpha = 10^{-3}, \beta = 1, 10, 100, 1000, 10,000$ and in (b) for fixed $\beta = 1, \alpha = 1, 10^{-9}, 10^{-8}, 10^{-7}$.

where K_m denotes hydraulic conductivity in matrix and ϵ represents constant distance associated with radius r_m. From Equations (33) and (34), we can write

$$\alpha = \frac{2K_m}{\epsilon r_c r_m}, \tag{35}$$

and from Equation (7)

$$\alpha_0 = \pi r_c^2 \alpha = \frac{2\pi K_m}{\epsilon \sqrt{\beta}}, \tag{36}$$

where α_0 is the one-dimensional exchange coefficient.

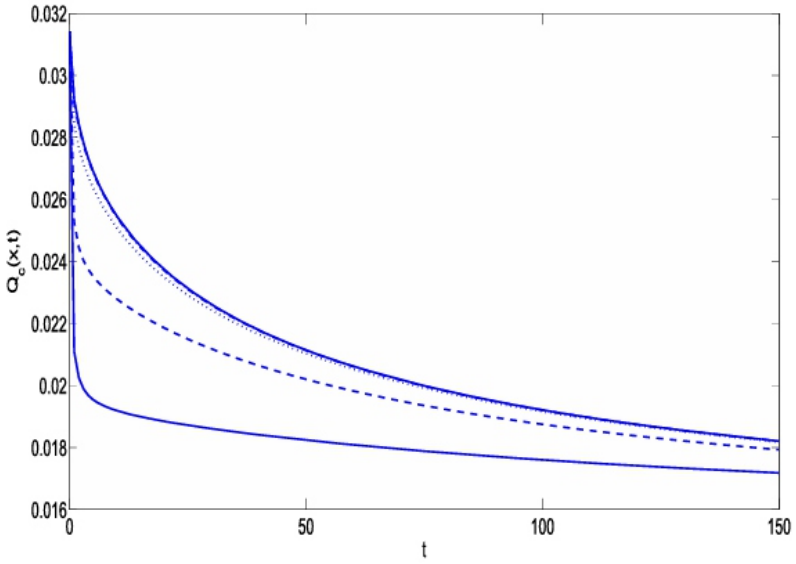

Figure 3. Simulated flow rate w.r.t. fixed coefficient $K_c = 10\,\mathrm{m}^3\,\mathrm{s}^{-1}, S_c = 5 \times 10^{-2}\,\mathrm{m}, S_m = 10^{-4}\,\mathrm{m}, x = 150\mathrm{m}, \eta = 1, \zeta = 1$ and for fixed $\alpha = 10^{-3}, \beta = 1, 10, 100, 1000, 10,000$.

In Figure 1, the behaviour of hydraulic head in channel continua with respect to time variable t is obtained by taking different parameters and fractional order to see the behaviour with integer order derivative. Figure 2 shows the behaviour of hydraulic head with respect to variations of the coefficient β and α.Fortheincreasingvaluesofβ taking fixed exchange rate between porosities i.e. for constant α the hydraulic head is decreased. Here β is affected in the same way as the storage coefficient and α does, so coefficient β is very useful in a dual-porosity model to simulate hydraulic head and flow [32]. Similarly, for the decreasing values of coefficient α taking β constant, hydraulic head varies as shown in Figure 3 shows the behaviour of flow rate with respect to time t taking fixed parameters.

6. Conclusion

The dual-porosity approach is used to analyse the hydraulic head in the karst aquifer for the non-integer differential equations by applying the Caputo–Fabrizio fractional operator. We use Laplace transform

on the modified governing differential equation to obtain the hydraulic head and connection between the channel and the matrix continua. The dualporosity approach enables inferences about karstic network structure and its effect on the hydraulic head. The governing differential equation for channel and matrix continua can be used to monitor the karstic structure and are appropriate for any transient boundary state. The models of dual-porosity transfer function allow inferences to be made about the structure of the karstic network and its impact on the spring hydrograph. The developed analytical models, valid foranytransientboundarycondition,canbeusedtoinvestigatethe karstic structure, homogeneous/heterogeneous infiltration processes, and parameter distribution impacts on the hydraulic responses of highly heterogeneous systems like karstic aquifers.

Acknowledgments

The authors express their sincere thanks to the reviewers for their careful reading and useful suggestions that helped to improve this paper.

Dataavailability statement

No data were used to support this study.

Disclosure statement

Nopotential conflict of interest was reported by the author(s).

ORCID

Mahaveer Prasad Yadav http://orcid.org/0000-0001-5657-3367
Ritu Agarwal http://orcid.org/0000-0002-8532-6696
Sunil Dutt Purohit http://orcid.org/0000-0002-1098-5961
Devendra Kumar http://orcid.org/0000-0003-4249-6326
Daya Lal Suthar http://orcid.org/0000-0001-9978-2177

References

[1] Mohrlok U, Sauter M. Modelling groundwater flow in a karst terrain using discrete and double-continuum approaches. Importance of spatial and temporal distribution of recharge. Proceedings of the 12th International Congress of Speleology; 6th Conference on Limestone Hydrology and Fissured Media; Vol. 2; 1997. p. 167–170.

[2] Mohrlok U, Teutsch G. Double-continuum porous equivalent (DCPE) versus discrete modelling in karst terraces. Karst Waters & Environmental Impacts; 1997. p. 319–326.

[3] Cornaton F, Perrochet P. Analytical 1D dual-porosity equivalent solutions to 3D discrete single-

-continuum models. Application to karstic spring hydrograph modelling. J Hydrol. 2002;262(1–4):165–176.

[4] Warren JE, Root PJ. The behaviour of naturally fractured reservoirs. Soc Pet Eng J. 1963;3:245–255.

[5] Kazemi H. Pressure transient analysis of naturally fractured reservoirs with uniform fracture distribution. Soc Pet Eng J. 1969;246:451–462.

[6] Moench AF. Double porosity models for a fractured groundwater reservoir with fracture skin. Water Resour Res. 1984;20(7):831–846.

[7] Barenblatt GI, ZheltovIP, KochinaIN. Basicconceptsinthetheoryofseepageofhomogeneous liquidsinfracturedrocks(strata). JApplMathMech. 1960;24(5):1286–1303.

[8] Lang U, Keim B. Modelling flow and transport processes in fractured or karstified media with a double continuum model. Abstracts of Conference MODFLOW'98; Golden, CO; 1998. p. 329–336.

[9] Moutsopoulos KN, Konstantinidis AA, Meladiotis ID, et al. On the numerical solution and qualitative behaviour of double porosity aquifers. Transp Porous Media. 2001;42:265–292.

[10] Pride SR, Berryman JG. Linear dynamics of double porosity dual-permeability materials. I. Governing equations and acoustic attenuation. Phys Rev E. 2003;68(36603):1–10.

[11] AgarwalR, YadavMP, BaleanuD, etal. Existenceanduniquenessofmiscibleflowequation through porous media with a non singular fractional derivative. AIMS Mathematics. 2020;5(2):1062–1073.

[12] Atangana A, Alkahtani BST. New model of groundwater flowing within a confine aquifer: application of Caputo-Fabrizio derivative. Arab J Geosci. 2016;9(1):8.

[13] Atangana A. On the new fractional derivative and application to nonlinear Fisher's reactiondiffusion equation. Appl Math Comput. 2016;273:948–956.

[14] Baleanu D, Rezapour S, Saberpour Z. On fractional integro-differential inclusions via the extended fractional Caputo-Fabrizio derivation. Boundary Value Problems. 2019;2019:79.

[15] Atangana A, Baleanu D. Caputo-Fabrizio derivative applied to groundwater flow within confined aquifer. J Eng Mech. 2017;143(5):D4016005.

[16] Yavuz M, Sene N, Yıldız M. Analysis of the influences of parameters in the fractional secondgrade fluid dynamics. Mathematics. 2022;10(7):1125.

[17] Hammouch Z, Yavuz M, Özdemir N. Numerical solutions and synchronization of a variableorder fractional chaotic system. Math Model Numer Simul Appl. 2021;1(1):11–23.

[18] Akgül EK, Akgül A, Yavuz M. New illustrative applications of integral transforms to financial models with different fractional derivatives. Chaos, Solitons & Fractals. 2021;146:110877.

[19] BaleanuD, EtemadS, PourraziS, etal. Onthenewfractionalhybridboundaryvalueproblems with three-point integral hybrid conditions. Adv Differ Equ. 2019;473:0.

[20] Baleanu D, Hassan Abadi M, Jajarmi A, et al. A new comparative study on the general fractional

model of COVID-19 with isolation and quarantine effects. Alexandria Eng J. 2022;61(6):4779–4791.

[21] Qureshi S, Rangaig NA, Baleanu D. New numerical aspects of Caputo-Fabrizio fractional derivative operator. Mathematics. 2019;7(4):374.

[22] Jajarmi A, Baleanu D, Zarghami Vahid K, et al. A new and general fractional Lagrangian approach:acapacitormicrophonecasestudy.ResultsPhys.2021;31:104950.

[23] Thabet STM, Etemad S, Rezapour S. On a coupled Caputo conformable system of pantograph problems. Turkish J Math. 2021;45:496.519.

[24] Matar MM, Abbas MI, Alzabut J, et al. Investigation of the p-Laplacian nonperiodic nonlinear boundary value problem via generalized Caputo fractional derivatives. Adv Differ Equ. 2021;68:0.

[25] AhmadM,ImranMA,AleemM,etal.Acomparativestudyandanalysisofnaturalconvection f low of MHD non-Newtonian fluid in the presence of heat source and first-order chemical reaction. J Therm Anal Calorim. 2019;137:1783–1796.

[26] Aleem M, Asjad MI, Shaheen A, et al. MHD influence on different water based nanofluids (TiO2, Al2O3,CuO)inporousmediumwithchemicalreactionandnewtonianheating.Chaos Solitons Fractals. 2020;130:109437.

[27] Asjad MI, Shah NA, Aleem M, et al. Heat transfer analysis of fractional second-grade fluid subject to Newtonian heating with Caputo and Caputo-Fabrizio fractional derivatives: a comparison. Eur Phys J Plus. 2017;132:340.

[28] Yang X, Srivastava HM, Tenreiro Machado JA. A new fractional derivative without singular kernel: application to the modelling of the steady heat flow. Therm Sci. 2015;20(2):753–756.

[29] YangX,FengY,Cattani C, et al. Fundamental solutions of anomalous diffusion equations with the decay exponential kernel. Math Methods Appl Sci. 2019;42(11):4054–4060.

[30] Yang X, Gao F, Ju Y, et al. Fundamental solutions of the general fractional-order diffusion equations. Math Methods Appl Sci. 2018;41(18):9312–9320.

[31] Caputo M, Fabrizio M. A new definition of fractional derivative without singular kernel. Prog Fract Differ Appl. 2015;2:73–85.

[32] Cornaton F. Utilisation de modèles continu discret et à double continuum pour l'analyse des réponsesglobalesdel'aquifèrekarstique.Essaid'identificationdesparamètres[MasterThesis]. University of Neuchâtel; 1999. p. 83.

Comparative analysis of FISTA and inertial Tseng algorithm for enhanced image restoration in prostate cancer imaging

AbubakarAdamua,b,HuzaifaUmara,SamuelEniolaAkinadecandDilberUzun Ozsahina,d,e

a Operational Research Centerin Healthcare, Near East University, Nicosia, Turkey; bCharles Chidume Mathematics Institute, African University of Science and Technology, Abuja, Nigeria; cDepartment of Mathematics, Illinois State University, Illinois, USA; dDepartment of Medical Diagnostic Imaging, College of Health Science, University of Sharjah, Sharjah, UAE; eResearch Institute for Medical and Health Sciences, University of Sharjah, Sharjah,UAE

A B S T R A C T

Thresholding Algorithm (FISTA) are well-established methods that provide effective ways to approximate zeros of the sum of monotone operators. In this study, we applied both ITA and FISTA in the

were degraded with known blur functions and additive noise. The

and prostate MRI pathology. Both algorithms incorporated the regularizer and l_1-regularizer. Numerical simulations revealed that the ITA method consistently outperforms the FISTA method in terms of image quality, despite FISTA's computational efficiency advantage. Additionally, the study found that, for both methods, images restored using the TV-regularizer exhibit higher quality compared to those restored using the l_2-regularizer. Overall, the study revealed the effectiveness of the algorithms employed and highlight the significance of integrating mathematical models with well established mechanism in medical image restoration.

KEYWORDS Medical image restoration; image deblurring; Tseng algorithm; prostatecancer; osteosarcoma

1. Introduction

Medical imaging plays a critical role in the diagnosis and treatment of various diseases, offering valuable insight to healthcare professionals. With the advancement of technology in the last decade, medical devices have been developed and become faster, more accurate, and less invasive [1]. Mathematical models are integral to medical image restoration, aiming to obtain high-quality images for clinical purposes and minimize risks and costs associated with patient care. Although data-driven models, especially deep models, are adept at extracting valuable insights from extensive datasets, they often lack solid theoretical foundations [2]. Therefore, mathematical models and data derived from images give an insight in biomedical diagnostics, which are essential components of experimental, clinical, biomedical, and behavioural research. Medical imaging plays a pivotal role in the diagnosis and treatment of various diseases, including cancer, offering valuable guid-

ance to healthcare professionals [3]. Mathematical models are incredibly important in the f ield of medical image restoration. They allow for the production of high-quality images that can be used for clinical purposes, all while minimizing risks and costs associated with patient care. Data-driven models, especially deep models, are particularly useful in extracting valuable insights fromlargedatasets. However,itisimportanttonotethattheymaynot always have robust theoretical foundations. Nonetheless, mathematical models are vital in the field of biomedical computing, with image data processing playing a critical role in clinical, biomedical, experimental, and behavioural research [4]. Prostate cancer (PC) is the most commonformofnon-skincancerfoundinmenacross various countries globally, including the United States [5, 6]. Globally, PC ranks as the fifth leading cause of male deaths related to cancer, resulting in approximately 350,000 deathsannually. IntheUnitedStates,itstandsasthesecondleadingcauseofcancer-related deaths among men [7]. The vast majority (90–95%) of diagnosed prostate cancer cases belong to the adenocarcinoma category. Adenocarcinoma is distinguished by elevated levels of prostate-specific antigen (PSA), which aids in the diagnostic process. Moreover, this form of cancer entails the expression or activation of the androgen receptor [8]. Approxi mately, 80% of clinically diagnosed cases of prostate cancer are localized and confined to the prostate gland, with the remaining 20% being metastatic [9]. PC screening is a highly controversial topic and remains one of themostdebatedissuesinhealthcare. Thoseagainst PSA screening express worries about over diagnosis of non-lethal cancers, which may lead to overtreatment, causing treatment-related side effects, psychological distress, and substantial medical costs [10]. Identifying biomarkers can enhancethediagnosisandtreatment of prostate cancer [11]. Measuring PSA concentration can aid in deciding whether a biopsy is necessary, potentially reducing morbidity [12].

Osteosarcomaisaclassic primary bonesarcomathatprimarilyaffects childrenandadolescents, and the typical characteristic of osteosarcoma is the productionofimmaturebone or osteoid tissue by malignant osteoblasts [13]. Individuals diagnosed with osteosarcoma frequently confront the possibility of relapse, with pulmonary metastasis emerging as the predominant site. Despite undergoing aggressive treatment, approximately one-third of patients initially diagnosed with osteosarcoma without metastasis encounter recurrence during follow-up periods [14]. In developing countries, osteosarcoma has an average incidence of 0.0003% and ranks as the most prevalent malignant bone tumour after multiple myeloma,representing0.2%ofmalignancies.Itshighmalignancyoftenleadstoearly-stage distant metastasis, with approximately 20% of patients already diagnosed with pulmonary metastasis at the time of diagnosis [15].

Magnetic resonance imaging (MRI) technology is commonly used for imaging inations related to cancer and other diseases [16]. Diagnosing osteosarcoma and prostate

cancerindevelopingcountriespresentssignificantchallenges.Inmanydevelopingnations, healthcare infrastructure is limited, and there is an imbalance in the doctor-to-patient ratio, making it hard to offer personalized and specialized medical services. The process of diagnosing and treating osteosarcoma is time-consuming and financially burdensome. Consequently, many impoverished families may have to forgo treatment due to the prohibitive costs involved [17]. Identifying osteosarcoma manually in MRI images poses a labour-intensive and time-consuming challenge for doctors due to the substantial volume of data and the complexity involved in detection. Moreover, the subjective nature of this process increases the likelihood of missed or misdiagnosed issues [18]. Therefore, there is need to develop a reliable mathematical algorithm that is capable of restoring images and accurately detecting various types of diseases.

Image restoration encompasses various techniques, including image denoising [19], deblurring [20], inpainting [21], dehazing [22], and de-raining [22]. In solving medical imaging analysis problems, numerical simulations are often preferred due to factors like specular noise that can impact image interpretation. Therefore, the study of medical images requires the use of complex mathematical models employing diverse algorithms. In this study, we employed two famous algorithms, the improvement of Fast Iterative Shrinkage-Thresholding Algorithm (FISTA) proposed by Liang et al. [23] and the Inertial Tseng Algorithms (ITA) proposed by Padcharaeon et al. [24], to restore MRI images of PC and osteosarcoma that were degraded with an additive noise and known blur functions. Additionally, We employed established image restoration tools to enhance the quality of the biomedical images and conducted comparisons between the algorithms used and the restored images with their original counterparts.

2. Methodology

The MRI images of PC and osteosarcoma were retrieved from the cancer imaging archive (https://www.cancerimagingarchive.net), which is an open-source licence (https://creativecommons.org/licenses/by/3.0/); they represent various disease conditions and ethical approval is not applicable. Many image restoration problems can be reformulated as convex optimization problems of the form:

$$\text{find } u \in \mathbb{R}^N \quad \text{such that } u = \arg\min_x \left\{ \frac{1}{2}\|Dx - \eta\|^2 + \mu G(x) \right\},$$

where D is a degradation function, x is the original image, η is noise, μ is a regularization parameter and G is a regularization function introduced due to the nature of the function (or matrix) D. In the literature, several regularization functions have been considered depending on the objective of the image restoration problem. One of the famous regulariz-

ers is the l_1-regularizer which usually appears in the l_1 regualarization problem, popularly known as least absolute shrinkage and selection operator (LASSO) problem which is to

$$\text{find } u \in \mathbb{R}^N \quad \text{such that } u = \arg\min_x \left\{ \frac{1}{2}\|Dx - \eta\|^2 + \mu\|x\|_{l_1} \right\}, \tag{1}$$

where $\|\cdot\|_{l_1}$ is the usual taxi-cab norm on $\mathbb{R}^N$ referred to as the l_1 regularization function. The l_1-regularizer is a powerful tool in image denoising and deblurring and has been explored by a host of many authors see, e.g. [23–27]

Another regularizer use for image restoration problems is the discrete Total Variation regularizer defined by

$$\|x\|_{\text{TV}} = \sum_{i=1}^{n-1}\sum_{j=1}^{m-1}\sqrt{(x_{i+1,j} - x_{i,j})^2 + (x_{i,j+1} - x_{i,j})^2}$$

$$+ \sum_{i=1}^{m-1}|x_{i,n} - x_{i+1,n}| + \sum_{j=1}^{n-1}|x_{m,j} - x_{m,j+1}|.$$

The TV-regularization problem is defined by

$$\text{find } u \in \mathbb{R}^N \quad \text{such that } u = \arg\min_x \frac{1}{2}\|Dx - \eta\|^2 + \mu\|x\|_{TV}. \tag{2}$$

This regularizer is known for restoring images with cartooning effects and edge-preserving properties. For more on regularizers used for image restoration problem interested readers may see [22].

All these regularization problems arising from image restoration can be reformulated as follows:

$$\text{find } u \in \mathbb{R}^N \quad \text{such that } u = \arg\min_x \left\{ h(x) + g(x) \right\}, \tag{3}$$

where

$$h(x) := \frac{1}{2}\|Dx - \eta\|^2 \quad \text{and} \quad g(x) := G(x), \text{ a regularization function.}$$

Through a simple mathematical reformulation, solutions to the minimization problems (3) are equivalent to solutions to the inclusion problem:

$$\text{find } u \in \mathbb{R}^N \quad \text{such that } 0 \in \left(\nabla f(u) + \partial g(u) \right), \tag{4}$$

where ∇f is the gradient of f and ∂g is the subdifferential of g, explicitly given as

$$\nabla f(x) = D^T(Dx - \eta) \quad \text{and} \quad \partial g(x) = \begin{cases} \dfrac{x}{\|x\|}, & x \neq 0; \\ \{x : \|x\| \leq 1\}, & x = 0. \end{cases}$$

In the literature, several algorithms have been introduced to approximate zeros of the sum of two monotone operators, which are frequently utilized to tackle the inclusion problem (4) (see, e.g. [28–34] and the references therein). We are interested in some recent methods developed based on the famous forward-backwards algorithm used for solving the inclusion problem (4), namely the ITA proposed by Padcharaeon et al. [24] and improving the FISTA proposed by Liang et al. [23] due to their efficiency in solving image restoration problems. We recall that the mathematical formulation for the image restoration problem is given by (5) and illustrated in Figure 1:

$$h = Ax + w, \tag{5}$$

where x is the original image, A is the degradation function, y is the observed image, and w is noise.

We will study the performance of the ITA of [23] and a new version FISTA by Liang et al. [23] in the restoration process of postrate cancer images that were initially degraded by random noise and motion blur. We will consider the discrete TV-regularization model (2) and the l_1-regularization model (1) to solve this problem. For completeness, we will

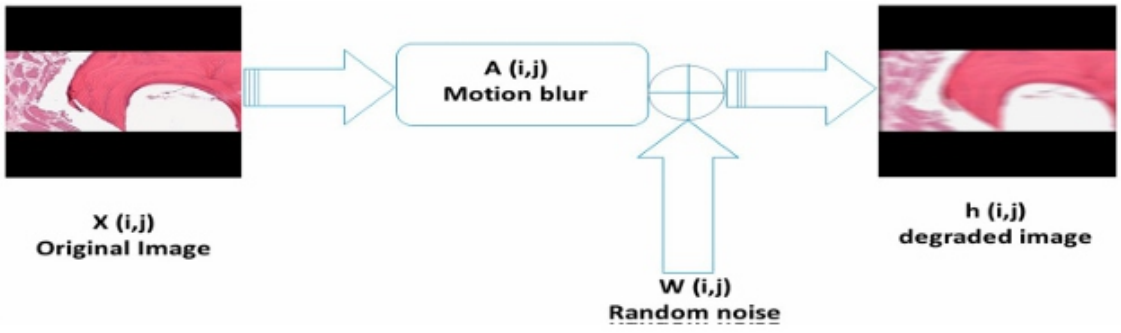

Figure 1. Image degradation process.

introduce the ITA and FISTA methods here without their respective convergence analy-

Algorithm 1: Inertial Tseng Algorithm (ITA) of Padcharaeon et al. [24]

Step 1. Given $x_0 = x_1 = Dx + \eta$, $\lambda_{TV} = 0.01$, $\mu = 0.3$ and $\alpha = 0.9$. Set $k = 1$.

Step 2. Compute x_{k+1}, w_k, and y_k via

where I is the identity mapping.

Step 3. Set $k \leftarrow k+1$, and **go to Step 2**.

Algorithm 2: Modified FISTA Method of Liang et al. [23] (FISTA)

Step 1. Given $x_0 = x_1 = Dx + \eta$, $\lambda_{TV} = 0.01$, $\mu = 0.3\, p = 1, q = 1.4, r = 4$ and $t_0 = 1$. Set $k = 1$.

Step 2. Compute t_k, a_k, y_k, w_k and x_{k+1} via

$$\begin{cases} t_k = \dfrac{p + \sqrt{q + rt_{k-1}}^2}{2}, \quad a_k = \dfrac{t_{k-1} - 1}{t_k}, \\ y_k = x_k + a_k(x_k - x_{k-1}), \\ w_k = (I + \lambda_{TV}\mu\partial g)^{-1}(y_k - \mu\nabla f(y_k)), \end{cases} \tag{7}$$

where I is the identity mapping.

Step 3. Set $k \leftarrow k+1$, and **go to Step 2**.

2.1. Convergence analysis

Theorem 2.1: *The sequence $\{x_k\}$ generated by Algorithms 1 and 2 converges to a solution of problem (3).*

Proof: Since ∇f is Lipschitz monotone, and ∂g is maximal monotone, the convergence analysis follows using a similar argument given in [23, 24], by setting $A = \nabla f$ and $B = \partial g$, in these references, respectively. ■

2.2. Experimental results and discussion

In this section, we will give a comparative study of Algorithms 1 and 2 in the restoration process of some prostate and osteosarcoma cancer images. We will consider four (4) test images, which we label as follows: Images 1, 2, 3 and 4, which are actually the original Osteosarcoma Tumour I, Osteosarcoma Tumour II, Prostate fused, and Prostate MRI pathology, respectively. The performance of Algorithms 1 and 2 in the restoration process of thesetest imagesthatwereinitiallydegradedusing'MATLAB'sbuilt-inmotionblur function' (P = fspecial(motion,30,60)) was studied, and Gaussian noise (GN) scaling

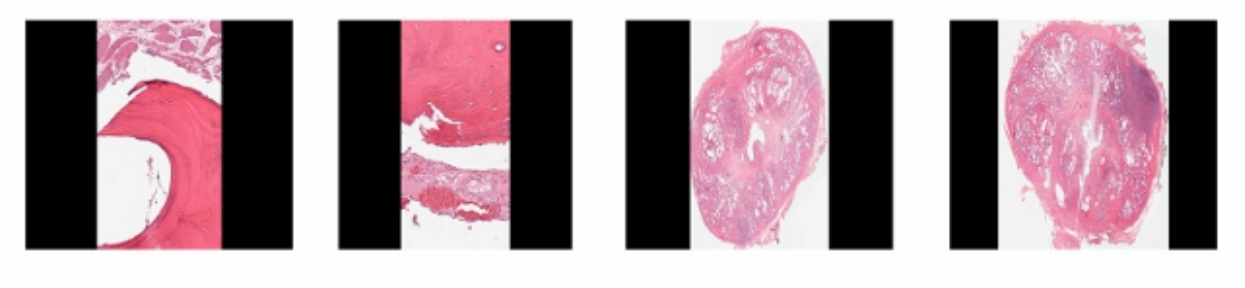

(a) original images

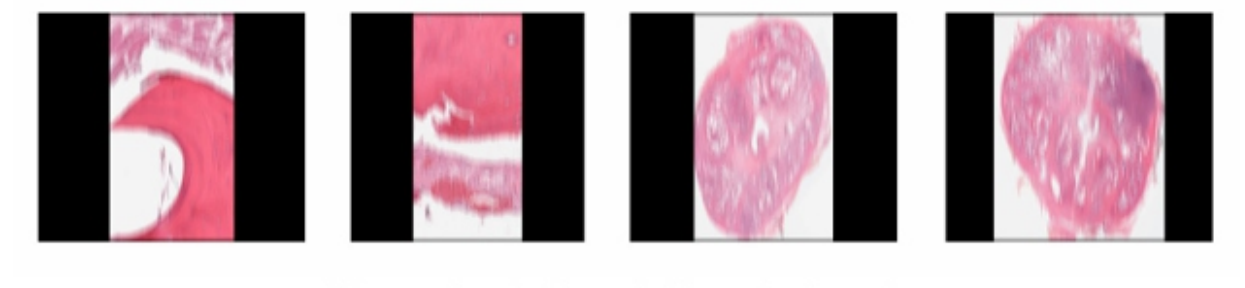

(b) images degraded by motion blur and random noise

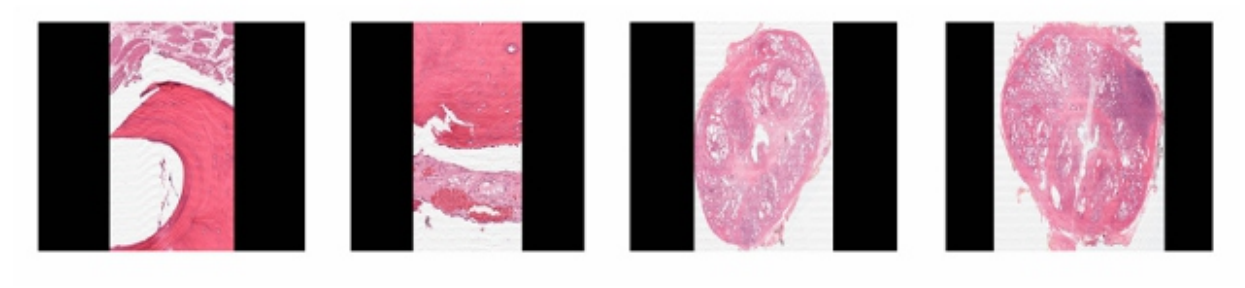

(c) restored images with ITA

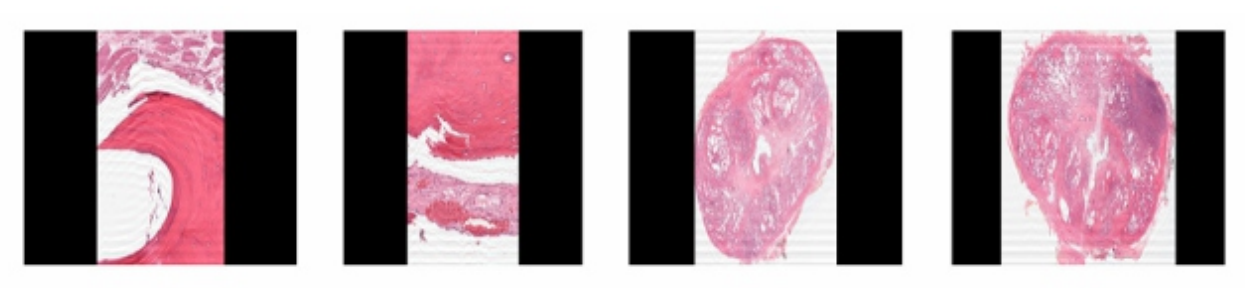

(d) restored images with FISTA

Figure 2. Test images and their restorations via ITA and FISTA using TV-regularizer. (a) original images.
(b) images degraded by motion blur and random noise. (c) restored images with ITA and (d) restored images with FISTA.

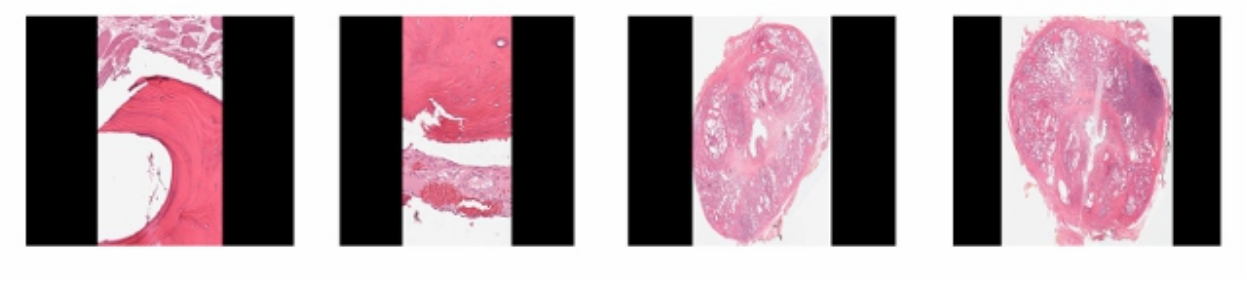

(a) original images

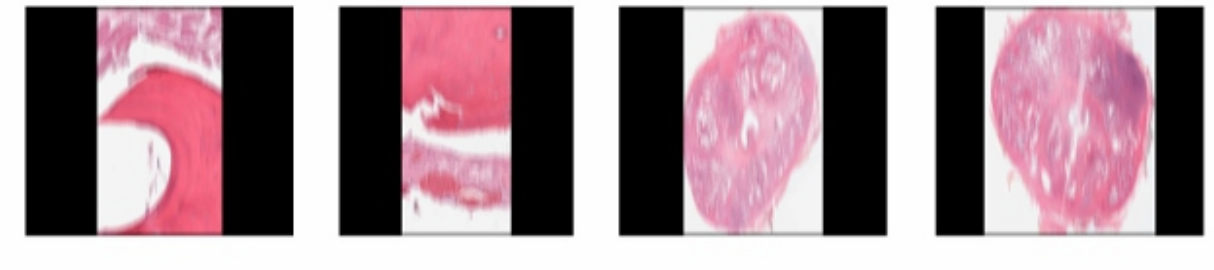

(b) images degraded by motion blur and random noise

(c) restored images with ITA

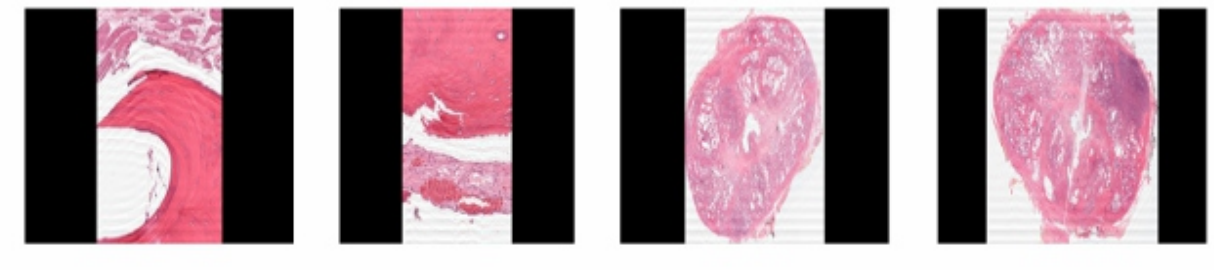

(d) restored images with FISTA

Figure 3. Test images and their restorations via ITA and FISTA l1-regularizer. (a) original images. (b) images degraded by motion blur and random noise.(c)restored images with ITA and (d)restored images with FISTA.

factor $\sigma = 0.001$ wasadded. Furthermore, TV-regularizer and the l1-regularizer was considered, and the effect of these regularizers when used in Algorithms 1 and 2 is studied. Theoutcomesofthesimulationsareshown inFigures2, 3, 4 and 5 below:

Discussion. Looking at the restored images via ITA and FISTA using TV-regularizer and l1-regularizer

(see Figures 2 and 3),weobserve that therestoredimagesviaTVregularizerappear tobemorecloser totheoriginal imagescomparedtotherestored images via l1-regularizer. Furthermore, the images restored using the ITA method appear to clearer than those restored using the FISTA method. However, we employed tools to

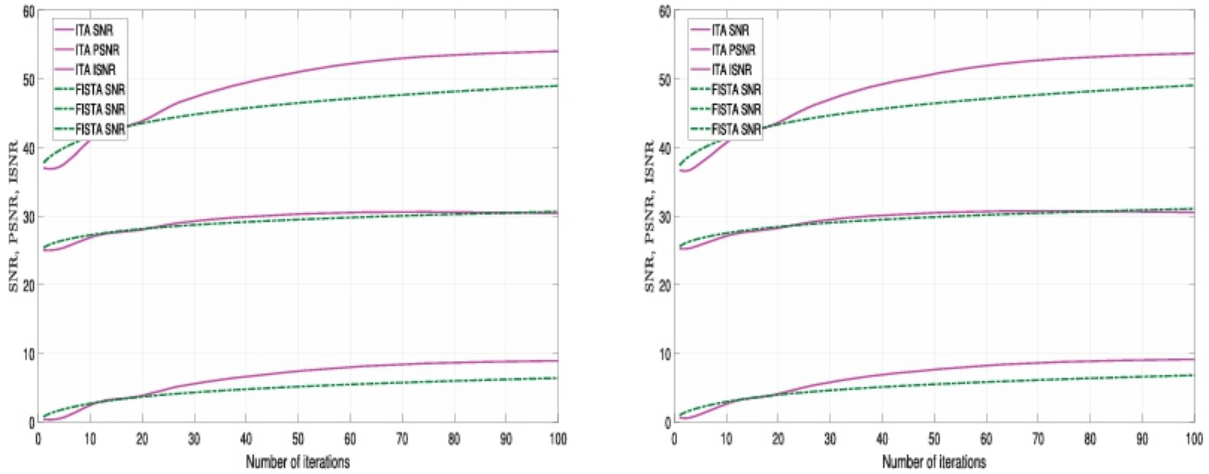

Figure 4. Graphical representation of the results in Table 1, Left: Image 1; Right: Image 2.

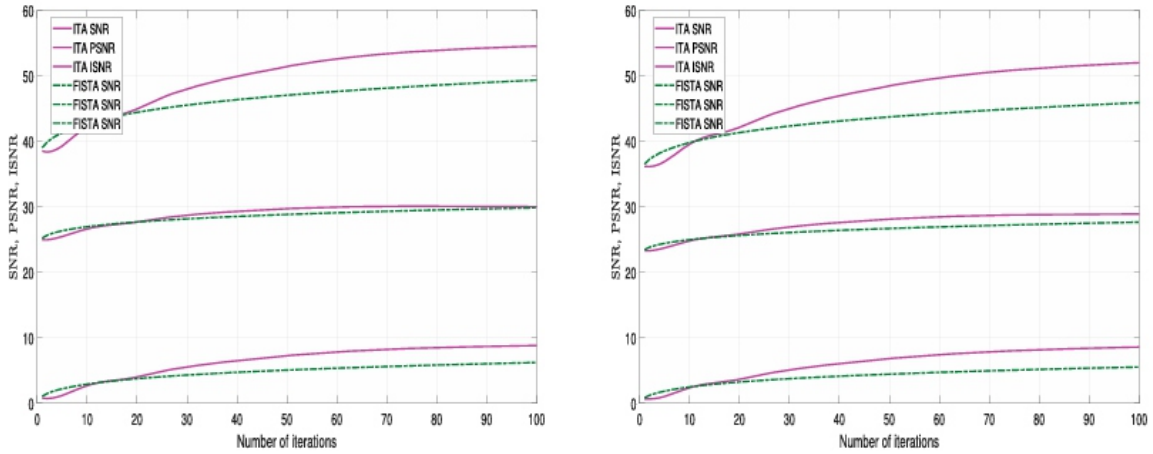

Figure 5. Graphical representation of the results in Table 1, Left: Image 3; Right: Image 4.

measure the quality of restored images in order to validate the claim. Three different metrics were used for this analysis: Improvement in signal-to-noise ratio (ISNR), peak signal-to-noise ratio (PSNR), and signal-to-noise ratio (SNR). These metrics are expressed as follows:

$$\text{ISNR} := 10\log\frac{\|x-y\|^2}{\|x-x_n\|}, \quad \text{PSNR} = 10\log_{10}\left(\frac{\text{MAX}^2}{\text{MSE}}\right) \text{ and SNR} := 10\log\frac{\|x\|}{\|x-x_n\|^2}, \tag{8}$$

wherey,x,andxn denote the observed, original, and estimated image satiterationn, respectively, and MAX is the maximum possible pixel value and MSE is the Mean Squared Error between the original and distorted images.

A higher values for ISNR and SNR indicate superior restoration. Also, a higher PSNR value implies lower distortion and better quality. The performance of ITA Algorithm 1 and FISTA Algorithm 2 using these metrics is detailed in Tables 1 and 2 and Figures 4 and 5.

Remark 2.1: FromTable 1and Figures 4and 5,weobservethatusingtheTV-regularizer, the quality of the restored images using ITA are higher than the quality of the restored.

Table1. PerformancemetricsforthetestimagesusingTVregularizer.

ISNR, PSNR, SNR and CPU time for the test images								
	ITA				FISTA			
Test images	ISNR	PSNR	SNR	CPU Time	ISNR	PSNR	SNR	CPU time
Image 1	8.91	30.43	54.23	435.22	6.39	30.65	49.00	317.51
Image 2	9.12	30.55	53.72	437.52	6.79	31.08	49.08	319.47
Image 3	8.82	30.02	54.53	437.66	6.24	29.86	49.35	320.28
Image 4	8.6	28.9	51.99	441.9	5.55	27.66	45.91	320.59

Table2. PerformancemetricsforthetestimagesusingI1-regularizer.

ISNR, PSNR, SNR and CPU time for the test images								
	ITA				FISTA			
Test Images	ISNR	PSNR	SNR	CPU Time	ISNR	PSNR	SNR	CPU time
Image 1	8.07	30.98	52.38	264.49	6.29	30.56	48.82	141.57
Image 2	8.42	32.01	52.33	249.14	6.65	30.94	48.80	130.13
Image 3	7.92	30.90	52.73	238.05	6.24	29.86	49.35	320.28
Image 4	7.47	29.01	49.75	234.67	5.43	27.54	45.66	133.31

\

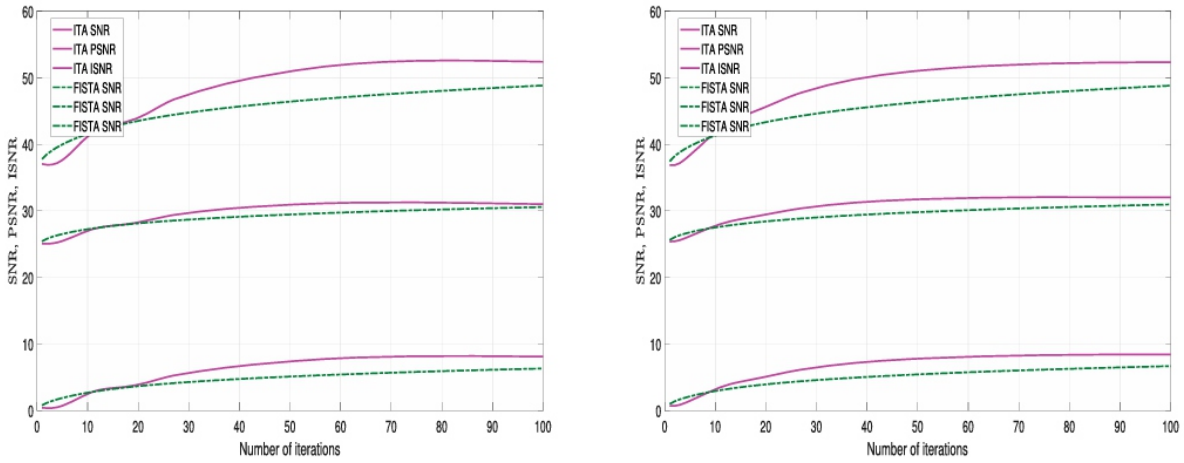

Figure6. Graphical representation of the results in Table2, Left: Image1; Right: Image2.

images using FISTA. But the computational time required to restore the images using FISTA is less than the computational time required using the ITA method. Hence, we deduce that in terms of quality ITA is better than FISTA and in terms of computational time, FISTA is better than ITA.

Remark 2.2: Also, from Table 2 and Figures 6 and 7, we observe that using the l_1-regularizer, the quality of the restored images using ITA are higher than the quality of the restored images using FISTA. But the computational time required to restore the images using FISTA is less than the computational time required using ITA method. Hence, we deduce that in-terms of quality ITA is better than FISTA and in terms of computational time, FISTA is better than ITA.

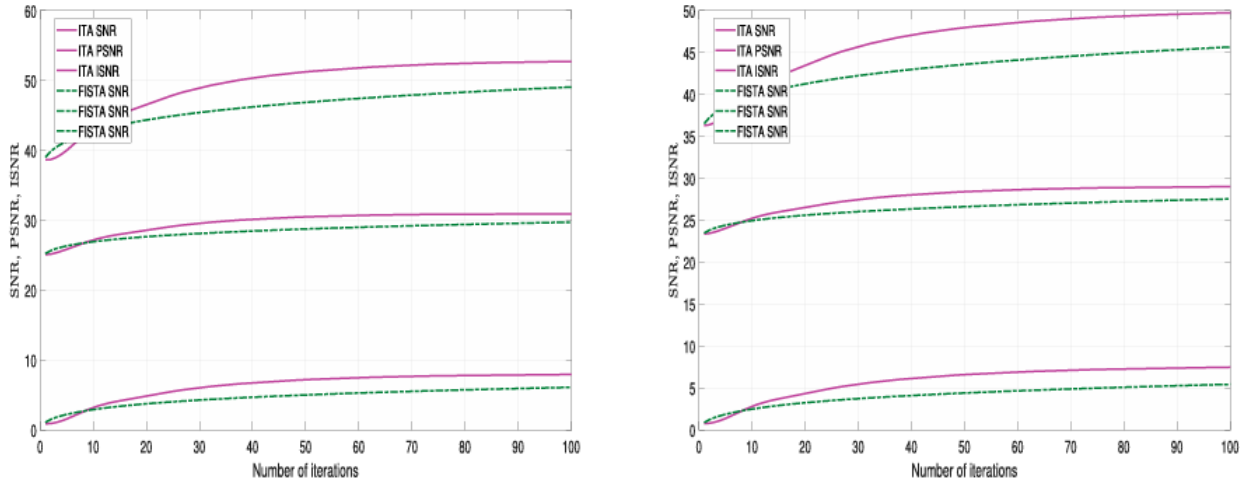

Figure 7. Graphical representation of the results in Table 2, Left: Image 3; Right: Image 4.

3. Conclusion

This study presents a comparative study of two famous Algorithms, namely, the inertial Tsengalgorithm(ITA)proposedbyPadcharaeonetal.[24]andimprovingtheFastIterative Shrinkage-ThresholdingAlgorithm(FISTA)proposedbyLiangetal.[23]intherestoration process of prostate cancer and osteosarcoma images that had been degraded with known blurfunctionandadditivenoise.Furthermore,theTV-regularizerandl1-regularizerswere used in each algorithm. The results of the numerical simulations suggest that the ITA method restores images with higher quality than the FISTA method, even though the FISTA method is less computationally expensive than the ITA method. Furthermore the qualityoftheimagesrestoredusingTV-regularizerishigherthanthequalityoftherestored images using l1-regularizer. However, the computational time for TV-regularizer is higher than that for l1-regularizer. Overall, this study successfully restored prostate cancer and osteosarcoma images that had been degraded with additive noise and a known blur. This approach revealed the potential of mathematical models when integrated with established toolsinmedicalimagerestoration,aswellastheefficacyofthealgorithms.

Acknowledgments

Theauthorsaregrateful for thesupportprovidedbytheirinstitutions. 'Operational Research Centre for Healthcare, Near East University, TRNC.' The author thank the anonymous reviewers for their esteemed comments and suggestions.

Disclosure statement

Nopotential conflict of interest was reported by the author(s).

Dataavailability statement

All data used in this study is included in the manuscript.

References

[1] Wang Y, Liu T. Quantitative susceptibility mapping (QSM): decoding MRI data for a tissue magnetic biomarker. Magn Reson Med. 2015;73(1):82–101. doi: 10.1002/mrm.v73.1

[2] Alvarez L, Guichard F, Lions PL, et al. Axiomes etequations fondamentales du traitement d'images. C R Acad Sci Paris. 1992;315:135–138.

[3] Chabat F, Hansell DM, Yang GZ. Computerized decision support in medical imaging. IEEE Eng MedBiol Mag. 2000;19(5):89–96. doi: 10.1109/51.870235

[4] Yan K, Wang X, Lu L, et al. DeepLesion: automated mining of large-scale lesion annotations and universal lesion detection with deep learning. J Med Imaging. 2018;5(3):036501–036501.

[5] RawlaP.Epidemiologyofprostate cancer. World J Oncol.2019;10(2):63–89. doi: 10.14740/wjon1191

[6] Siegel RL, Miller KD, Fuchs HE, et al. Cancer statistics, 2021. CA Cancer J Clin. 2021;71(1):7–33. doi: 10.3322/caac.v71.1

[7] RebelloRJ,OingC,KnudsenKE, etal.Prostatecancer.NatRevDisPrimers. 2021;7(1):9. doi: 10.1038/s41572-020-00243-0

[8] WangY,WangY,CiX,etal.Molecularеventsinneuroendocrineprostate cancer development. Nat Rev Urol. 2021;18(10):581–596. doi: 10.1038/s41585-021-00490-0

[9] SandhuS,MooreCM,ChiongE,etal.Prostatecancer.Lancet.2021;398(10305):1075–1090. doi: 10.1016/S0140-6736(21)00950-8

[10] Dunn MW. Prostate cancer screening. Semin Oncol Nurs. 2017;33(2):156–164. doi: 10.1016/j.soncn.2017.02.003

[11] Ferro M, Buonerba C, Terracciano D, et al. Biomarkers in localized prostate cancer. Future Oncol. 2016;12(3):399–411. doi: 10.2217/fon.15.318

[12] Nordstrom T, Akre O, Aly M. Prostate-specific antigen (PSA) density in the diagnostic algorithm of prostate cancer. Prostate Cancer Prostatic Dis. 2018;21:57–63. doi: 10.1038/s41391-017-0024-7

[13] Lee SL. Complications of radioactive iodine treatment of thyroid carcinoma. J Natl Compr Cancer Netw. 2010;8(11):1277–1286. doi: 10.6004/jnccn.2010.0094

[14] Kansara M. Translational biology of osteosarcoma. Nat Rev Cancer. 2014;14(11):722–735. doi: 10.1038/nrc3838

[15] OuyangT,YangS,GouF,etal.RethinkingU-netfromanattentionperspectivewithtransformers for osteosarcoma MRI image segmentation. Comput Intell Neurosci. 2022;2022:7973404. doi: 10.1155/2022/7973404

[16] Lv B, Liu F, Gou F, et al. Multi-scale tumor localization based on priori guidancebased segmentation method for osteosarcoma MRI images. Mathematics. 2022;10(12):2099. doi: 10.3390/math10122099

[17] Yu G, Chen Z, Wu J, et al. Medical decision support system for cancer treatment in cision medicine in developing countries. Expert Syst Appl. 2021;186:115725. doi: 10.1016/j.eswa.2021.115725

[18] Veeresha P, Ilhan E, Prakasha D, et al. Regarding on the fractional mathematical model of tumour invasion and metastasis. Comput Model Eng Sci. 2021;127:1013–1036.

[19]MamaevNV, YurinDV, KrylovAS. Finding the parameters of a nonlinear diffusion denoising method by ridge analysis. Comput Math Model. 2018;29:334–343. doi: 10.1007/s10598-018-9413-6

[20] Pang Z-F, Zhang H-L, Luo S, et al. Image denoising based on the adaptive weighted TV regularization. Signal Process. 2020;167:107325. doi: 10.1016/j.sigpro.2019.107325

[21] AbbassM,KimH,AbdelwahabS,etal.Imagedeconvolutionusinghomomorphictechnique. Signal

Image Video Process. 2019;13(4):703–709. doi: 10.1007/s11760-018-1399-1

[22] Liu L, Pang Z-F, Duan Y.Retinex based on exponent-type total variation scheme. Inverse Prob Imaging. 2018;12(5):1199–1217. doi: 10.3934/ipi.2018050

[23] Liang J, Luo T, Schonlieb C-B. Improving fast iterative shrinkage-thresholding algorithm: faster,smarter,andgreedier.SIAMJSciComput.2022;44(3):A1069–A1091. doi: 10.1137/21M1395685

[24] Padcharoen A, Kitkuan D, Kumam W, et al. Tseng methods with inertial for solving inclusion problems and application to image deblurring and image recovery problems. Comput Math Methods. 2021;3:1–14. doi: 10.1002/cmm4.v3.3

[25] Kitkuan D, Kumam P, Padcharoen A, et al. Algorithms for zeros of two accretive operators for solving convex minimization problems and its application to image restoration problems. J Comput Appl Math. 2019;354:471–495. doi: 10.1016/j.cam.2018.04.057

[26] Adamu A, Kitkuan D, Padcharoen A, et al. Inertial viscosity-type iterative method for solving inclusion problems with applications. Math Comput Simul. 2022;194:445–459. doi: 10.1016/j.matcom.2021.12.007

[27] DeephoJ,AdamuA,IbrahimAH,etal.Relaxedviscosity-typeiterativemethodswithapplication to compressed sensing. J Anal. 2023;31(3):1987–2003. doi: 10.1007/s41478-022-00547-2

[28] AdamuA,DeephoJ,IbrahimAH,etal.Approximationofzerosofsumofmonotonemappings with applications to variational inequality and image restoration problems. Nonlinear Funct Anal Appl. 2021;26(2):411–432.

[29] Adamu A, Kitkuan D, Kumam P, et al. Approximation method for monotone inclusion problems in real Banach spaces with applications. J Inequal Appl. 2022;2022(1):70. doi: 10.1186/ s13660-022-02805-0

[30] ChidumeCE,AdamuA,KumamP,etal.Generalizedhybridviscosity-type forward-backward splitting method with application to convex minimization and image restoration problems. Numer Funct Anal Optim. 2021;42:1586–1607. doi: 10.1080/01630563.2021.1933525

[31] Dechboon P, Adamu A, Kumam P. A generalized Halpern-type forward-backward splitting algorithm for solving variational inclusion problems. AIMS Math. 2023;8(5):11037–11056. doi: 10.3934/math.2023559

[32] Muangchoo K, Adamu A, Ibrahim AH, et al. An inertial Halpern-type algorithm involving monotone operators on real Banach spaces with application to image recovery problems. ComputApplMath.2022;41:364. doi: 10.1007/s40314-022-02064-1

[33] Lions PL, Mercier B. Splitting algorithms for the sum of two nonlinear operators. SIAM J Numer Anal. 1979;16(6):964–979. doi: 10.1137/0716071

[34] Tseng P. A modified forward-backward splitting method for maximal monotone mappings. SIAM J Control Optim. 2000;38(2):431–446. doi: 10.1137/S0363012998338806

On degenerate multi-poly-derangement polynomials and numbers

Sang JoYuna and Jin-WooParkb
aDepartment of Information Science and Mathematics, Dong-A University, Busan, Republic of Korea;
bDepartment of Mathematics Education, Daegu University, Gyeongsangbuk-do, Republic of Korea

A B S T R A C T

The problem of counting derangements was begun in 1708 by Pierre R´ emond de Montmort (see [Carlitz. The number of derangements of a sequence with given specification. Fibonacci Quart. 1978;16:255–258], [Clarke and Sved. Derangements and Bell numbers. Math Mag. 1993;66:299–303]), and its applications have been investigated actively by many researchers. In this paper, we study properties of the degenerate multi-poly-derangement polynomials and numbersthat are defined by using the multiple logarithm function, and derive some interesting identities related to these polynomials and numbers.

KEYWORDS Derangement polynomials; multiple logarithm; the Stirling number of the first kind and the second kind; λ-analogue of the Stirling numbers ofthe first and the second kind; degenerate exponential functions

1. Introduction

Let X be a set with n elements, say $X = \{1, 2, \ldots, n\}$. A permutation $1, 2, \ldots, n$ of X in which i is not placed in the ith place for each i is called a *derangement*. In other word, a derangement is a permutation with no fixed point. The number of derangements of X is called the nth *derangement number* and denoted by D_n. The nth derangement number is given by

$$D_n = n! \sum_{k=0}^{n} \frac{(-1)^k}{k!}, \quad \text{(see [1, 2])}. \tag{1}$$

By (1), the generating function of the derangement numbers is

$$\sum_{n=0}^{\infty} D_n \frac{t^n}{n!} = \frac{1}{1-t} \mathrm{e}^{-t}. \tag{2}$$

As a natural extension, Kim et al. defined the *derangement polynomials* by the generating function to be

$$\sum_{n=0}^{\infty} d_n(x)\frac{t^n}{n!} = \frac{1}{1-t}\,\mathrm{e}^{-1}\,\mathrm{e}^{xt}, \quad \text{(see [3–6])}. \tag{3}$$

When $x = 0$, $d_n(0) = D_n$ is the nth derangement numbers.

The problem of counting derangements was initiated by Pierre Rémond de Montmort in 1708 (see [1]). In [7], Clarke-Sved found some finite sum identities that include derangement numbers, binomial coefficients, Bell numbers and polynomials in general form. In [8], Du-Fonseca found the relationship between the derangement numbers and the Bernoulli numbers. Zhang-Gray–Wang–Zhang investigated the connections between combinatorial objects, for example, the number of derangements and many other permutations under various constraints, and gave bijective proofs in [9]. In [10], Elizalde gave another arguably simpler bijective proof of the recurrence relation $D_n = nD_{n-1} + (-1)^n$ for $(n \geq 1)$. Ryoo gave the differential equations that occur in the generating function of the derangement polynomials, and studied a survey of the distribution of zeros of derangement polynomials in [11].

For a given integer k, the *polylogarithm function* is defined by

$$Li_k(x) = \sum_{n=1}^{\infty} \frac{x^n}{n^k}, \quad \text{(see [12, 13])}. \tag{4}$$

And for nonzero integers n and k with $n \geq k$, the *Stirling numbers of the first kind* $S_1(n,k)$ and the *Stirling numbers of the second kind* $S_2(n,k)$ are defined by the generating function to be

$$(x)_n = \sum_{k=0}^{n} S_1(n,k)x^k \text{and} x^n = \sum_{k=0}^{n} S_2(n,k)(x)_k, \quad \text{(see [2])}, \tag{5}$$

where $(x)_0 = 1$, $(x)_n = x(x-1)\cdots(x-n+1)$, $(n \geq 1)$.

As a generalizations of polylogarithm function, Kim and Kim [14] defined the *multiple polylogarithm* as follows: For given integers $k_1, k_2, \ldots, k_r$,

$$Li_{k_1,k_2,\ldots,k_r}(x) = \sum_{0<n_1<n_2<\cdots<n_r} \frac{x^{n_r}}{n_1^{k_1} n_2^{k_2} \cdots n_r^{k_r}}, \quad (|x| < 1). \tag{6}$$

(see [14–18]). By (6), we see that

$$\begin{aligned} Li_{\underbrace{1,\ldots,1}_{r-times}}(t) &= \frac{(-1)^r}{r!}\big(\log(1-t)\big)^r, \quad (r \in \mathbb{N}), \\ &= \sum_{l=r}^{\infty} S_1(l,r)(-1)^{l-r}\frac{t^l}{l!}, \quad \text{(see 15)}. \end{aligned} \tag{7}$$

The extensions of some special functions by using (multiple) polylogarithm or (multiple) polyexponential functions have been defined and the properties of those functions have been investigated by many researchers (see [12–17,19–25]).

For any $\lambda \in \mathbb{R} - \{0\}$, the *degenerate exponential function* is defined to be

$$e_\lambda^x(t) = (1+\lambda t)^{\frac{x}{\lambda}},\ e_\lambda(t) = (1+\lambda t)^{\frac{1}{\lambda}}, \quad \text{(see [26, 27, 28])}. \tag{8}$$

The degenerates of special polynomials and numbers started with the pioneering work of Carlitz on the degenerate Bernoulli and degenerate Euler polynomials (see [28]), and by the degenerate exponential function, many degenerate versions of special polynomials have been defined and properties of these polynomials have beeen investigated by many researchers (see [1,3,15–17,21–37]). Kim et al. considered the degenerate versions of r-Bell polynomials, two variable Fubini polynomials and r-Stirling numbers of the second kind in [34]. In [36], authors gave a degenerate poly-Daehee polynomials as a generalization of the Daehee polynomials and found relationships between the sepolynomialsandsomespecial polynomials. Kim and Kim defined the degenerate Bell polynomials and found some identities for the degenerate Bell polynomials which answered to the relationship between two different types of degenerate Bell polynomials (see [32]). In [29], Khan et al. defined the degenerate Apostol-type polynomials of order α and gave some summation formulas, recurrences, differential equations, and explicit formulas for these polynomials. In [17], Kimetal.definedthemulti-poly-Euler–Genocchipolynomialsandfoundsomeinteresting identities of these polynomials.

As an extension of derangement polynomials, Kim considered the degenerate higher order derangement polynomials which are given by

$$\sum_{n=0}^{\infty} d_{n,\lambda}^{(r)}(x)\frac{t^n}{n!} = \frac{1}{(1-t)^r}\, e^{x-r}(t), \quad \text{(see [30])}. \tag{9}$$

In the special case $r = 1$, $d_{n,\lambda}(x) = d_{n,\lambda}^{(1)}(x)$ are called the *degenerate derangement polynomials* which are defined by Kim et al. in [35].

As a degenerate version of the Stirling numbers, the *λ-analogue of the Stirling numbers of the first kind* and *the second kind* $S_\lambda^{(1)}(n,k)$ and $S_\lambda^{(2)}(n,k)$, respectively, are defined by

$$(x)_{n,\lambda} = \sum_{k=0}^{n} S_\lambda^{(1)}(n,k)x^k \quad \text{and} \quad x^n = \sum_{k=0}^{n} S_\lambda^{(2)}(n,k)(x)_{k,\lambda}, \ \text{(see 26, 33)}, \tag{10}$$

where $(x)_{0,\lambda} = 1$ and $(x)_{n,\lambda} = x(x-\lambda)(x-2\lambda)\cdots(x-(n-1)\lambda)$, $(n \geq 1)$.

In this paper, we define the degenerate multi-poly-derangement polynomials and numbers by using multiple logarithm function, and derive some interesting identities related to

the falling factorial sequences, the Stirling numbers of the second kind, the λ-analogue of the Stirling numbers of the first kind and these polynomials and numbers.

2. Main results

In this section, we consider the *degenerate multi-poly-derangement polynomials* which is given by

$$\frac{r!Li_{k_1,\dots,k_r}\left(1-\mathrm{e}^{-t}\right)}{t^r(1-t)^r}\,\mathrm{e}^{x-r}(t)=\sum_{n=0}^{\infty} d_{n,\lambda}^{(k_1,\dots,k_r)}(x)\frac{t^n}{n!}. \tag{11}$$

In the special case $x=0$, $d_{n,\lambda}^{(k_1,\dots,k_r)}=d_{n,\lambda}^{(k_1,\dots,k_r)}(0)$ are called the *degenerate multi-poly-derangement numbers*.

By (7) and the definition of multi-poly-derangement polynomials, we see that

$$d_{n,\lambda}^{(\overbrace{1,\dots,1}^{r-times})}(x)=d_{n,\lambda}^{(r)}(x).$$

By (11), we get

$$\begin{aligned}\sum_{n=0}^{\infty} d_{n,\lambda}^{(k_1,\dots,k_r)}(x)\frac{t^n}{n!}&=\frac{r!Li_{k_1,\dots,k_r}\left(1-\mathrm{e}^{-t}\right)}{t^r(1-t)^r}\,\mathrm{e}^{x-r}(t)\\&=\left(\sum_{n=0}^{\infty} d_{n,\lambda}^{(k_1,\dots,k_r)}\frac{t^n}{n!}\right)\left(\sum_{n=0}^{\infty}(x-r)_{n,\lambda}\frac{t^n}{n!}\right)\\&=\sum_{n=0}^{\infty}\left(\sum_{m=0}^{n}\binom{n}{m}d_{n-m,\lambda}^{(k_1,\dots,k_r)}(x-r)_{m,\lambda}\right)\frac{t^n}{n!},\end{aligned} \tag{12}$$

and, by (10) and (12), we obtain the following theorem.

and, by (10) and (12), we obtain the following theorem.

Theorem 2.1: *For each nonnegative integer n, we have*

$$\begin{aligned}d_{n,\lambda}^{(k_1,\dots,k_r)}(x)&=\sum_{m=0}^{n}\binom{n}{m}d_{n-m,\lambda}^{(k_1,\dots,k_r)}(x-r)_{m,\lambda}\\&=\sum_{m=0}^{n}\sum_{l=0}^{m}\binom{n}{m}d_{n-m,\lambda}S_{\lambda}^{(1)}(m,l)(x-m)^k.\end{aligned}$$

Since

$$(a+b)^{-k}=\sum_{m=0}^{\infty}(-1)^m\binom{k+m-1}{m}a^m b^{n-m}, \tag{13}$$

by the definition of degenerate multi-poly-derangement polynomials and (13), we get

$$\begin{aligned}
\sum_{n=0}^{\infty} d_{n,\lambda}^{(k_1,\dots,k_r)}(x)\frac{t^n}{n!} &= \frac{r!}{t^r(1-t)^r}Li_{k_1,\dots,k_r}\left(1-\mathrm{e}^{-t}\right)\mathrm{e}^{x-r}(t)\\
&= \frac{r!\,\mathrm{e}^{x-r}(t)}{t^r(1-t)^r}\sum_{0<n_1<\cdots<n_{r-1}}\frac{1}{n_1^{k_1}\cdots n_{r-1}^{k_{r-1}}}\sum_{n_r=n_{r-1}+1}^{\infty}\frac{\left(1-\mathrm{e}^{-t}\right)^{n_r}}{n_r^{k_r}}\\
&= \sum_{n_r=1}^{\infty}\frac{\left(1-\mathrm{e}^{-t}\right)}{(n_r+n_{r-1})^{k_r}}\frac{r!\,\mathrm{e}^{x-r}(t)}{t^r(1-t)^r}\sum_{0<n_1<\cdots<n_{r-1}}\frac{\left(1-\mathrm{e}^{-t}\right)^{n_{r-1}}}{n_1^{k_1}n_2^{k_2}\cdots n_{r-1}^{k_{r-1}}}\\
&= \sum_{m=0}^{\infty}(-1)^m\binom{k_r+m-1}{m}n_r^{-k_r-m}\sum_{l=1}^{\infty}\sum_{n_r=1}^{l}S_2(l,n_r)(-1)^{l-n_r}n_r!\frac{t^l}{l!}\\
&\quad\times\frac{r\,\mathrm{e}^{-1}(t)}{t(1-t)}\frac{(r-1)!\,\mathrm{e}^{x-r+1}(t)}{t^{r-1}(1-t)^{r-1}}\sum_{0<n_1<\cdots<n_{r-1}}\frac{\left(1-\mathrm{e}^{-t}\right)^{n_{r-1}}}{n_1^{k_1}\cdots n_{k-1}^{k_{r-1}-m}}\\
&= r\left(\sum_{l=0}^{\infty}\sum_{n_r=1}^{l+1}\sum_{m=0}^{\infty}\binom{k_r+m-1}{m}\frac{(-1)^{l+1+n_r+m}n_r^{-k_r-m}S_2(l+1,n_r)n_r!}{l+1}\frac{t^l}{l!}\right)\\
&\quad\times\left(\sum_{n=0}^{\infty}d_{n,\lambda}\frac{t^n}{n!}\right)\left(\sum_{n=0}^{\infty}d_{n,\lambda}^{(k_1,\dots,k_{r-1}-m)}(x)\frac{t^n}{n!}\right)\\
&= \sum_{n=0}^{\infty}\left(\sum_{b=0}^{n}\sum_{l=0}^{b}\sum_{n_r=1}^{l+1}\sum_{m=0}^{\infty}r\binom{n}{b}\binom{b}{l}\binom{k_r+m-1}{m}\right.\\
&\quad\left.\times\frac{(-1)^{l+1+n_r+m}n_r!S_2(l+1,n_r)}{(l+1)n_r^{k_r+m}}d_{n-b,\lambda}d_{b-l,\lambda}^{(k_1,\dots,k_{r-1}-m)}(x)\right)\frac{t^n}{n!}.
\end{aligned}\tag{14}$$

By (14), we obtain the following theorem.

Theorem 2.2: *For each nonnegative integer n, we have*

$$\begin{aligned}
d_{n,\lambda}^{(k_1,\dots,k_r)}(x) &= \sum_{b=0}^{n}\sum_{l=0}^{b}\sum_{n_r=1}^{l+1}\sum_{m=0}^{\infty}r\binom{n}{b}\binom{b}{l}\binom{k_r+m-1}{m}\\
&\quad\times\frac{(-1)^{l+1+n_r+m}n_r!S_2(l+1,n_r)}{(l+1)n_r^{k_r+m}}d_{n-b,\lambda}d_{b-l,\lambda}^{(k_1,\dots,k_{r-1}-m)}(x).
\end{aligned}$$

Replacing k_r by $-k_r$. Since

$$\binom{-k_r+m-1}{m} = (-1)^m \binom{k_r}{m}, \tag{15}$$

by Theorem 2.2 and (15), we obtain the following corollary.

Corollary 2.3: *For each nonnegative integer n, we have*

$$d_{n,\lambda}^{(k_1,\ldots,k_r)}(x) = \sum_{b=0}^{n}\sum_{l=0}^{b}\sum_{n_r=1}^{l+1}\sum_{m=0}^{\infty} r\binom{n}{b}\binom{b}{l}\binom{k_r}{m} \times \frac{(-1)^{l+1+n_r} n_r! S_2(l+1,n_r)}{(l+1)n_r^{k_r+m}} d_{n-b,\lambda} d_{b-l,\lambda}^{(k_1,\ldots,k_{r-1}-m)}(x).$$

By (11), we get

$$\sum_{n=0}^{\infty}\left(d_{n,\lambda}^{(k_1,\ldots,k_r)}(x+1) - d_{n,\lambda}^{(k_1,\ldots,k_r)}(x)\right)\frac{t^n}{n!} = \frac{r!}{t^r(1-t)^r}\,\mathrm{e}^{x-r}(t)\,(e_\lambda(t)-1)\,Li_{k_1,\ldots,k_r}\left(1-\mathrm{e}^{-t}\right)$$

$$= \frac{r}{t}\left(\frac{1}{1-t}\,\mathrm{e}^{-1}(t)\right)\left(\frac{(r-1)!\,\mathrm{e}^{x-r+1}(t)}{t^{r-1}(1-t)^{r-1}}\right)(e_\lambda(t)-1) \times \sum_{0<n_1<\cdots<n_{r-1}} \frac{\left(1-\mathrm{e}^{-t}\right)^{n_{r-1}}}{n_1^{k_1}\cdots n_{r-1}^{k_{r-1}}} \sum_{n_r=1}^{\infty}\frac{\left(1-\mathrm{e}^{-t}\right)^{n_r}}{(n_r+n_{r-1})^{k_r}}$$

$$= \sum_{l=1}^{\infty}\sum_{n_r=1}^{l}\sum_{m=0}^{\infty}(-1)^{m+l+n_r}\binom{k_r+m-1}{m} n_r! n_r^{-k_r-m} S_2(l,n_r)\frac{t^l}{l!} \times \frac{r}{t}\left(\frac{\mathrm{e}^{-1}(t)}{1-t}\right)\left(\frac{(r-1)!}{t^{r-1}(1-t)^{r-1}}\,\mathrm{e}^{x-(r-1)}(t) \sum_{0<n_1<\cdots<n_{r-1}} \frac{\left(1-\mathrm{e}^{-t}\right)^{n_{r-1}}}{n_1^{k_1}\cdots n_{r-1}^{k_{r-1}-m}}\right)$$

$$= \sum_{l=0}^{\infty}\left(\sum_{n_r=1}^{l+1}\sum_{m=0}^{\infty}(-1)^{m+l+1+n_r}\binom{k_r+m-1}{m}\frac{n_r! n_r^{-k_r-m} S_2(l+1,n_r)}{l+1}\frac{t^l}{l!}\right) \times r\left(\sum_{n=0}^{\infty} d_{n,\lambda}\frac{t^n}{n!}\right)\left(\sum_{n=1}^{\infty}(1)_{n,\lambda}\frac{t^n}{n!}\right)\left(\sum_{n=0}^{\infty} d_{n,\lambda}^{(k_1,\ldots,k_{r-1}-m)}(x)\frac{t^n}{n!}\right)$$

$$= \sum_{n=1}^{\infty}\left(r\sum_{l=0}^{n}\sum_{b=1}^{n-l}\sum_{a=1}^{b}\sum_{n_r=1}^{l+1}\sum_{m=0}^{\infty}\binom{n}{l}\binom{n-l}{b}\binom{b}{a}\binom{k_r+m-1}{m}(1)_{a,\lambda}\right.$$

$$\times \frac{(-1)^{m+l+1+n_r} n_r! S_2(l+1,n_r)}{(l+1)n_r^{k_r+m}} d_{b-a,\lambda} d_{n-l-b,\lambda}^{(k_1,\ldots,k_{r-1}-m)}(x)\Bigg)\frac{t^n}{n!}. \tag{16}$$

By (16), we obtain the following theorem.

Theorem 2.4: *For each nonnegative integer n, we have*

$$\begin{aligned} & d_{n,\lambda}^{(k_1,\ldots,k_r)}(x+1) - d_{n,\lambda}^{(k_1,\ldots,k_r)}(x) \\ &= r\sum_{l=0}^{n}\sum_{b=1}^{n-l}\sum_{a=1}^{b}\sum_{n_r=1}^{l+1}\sum_{m=0}^{\infty}\binom{n}{l}\binom{n-l}{b}\binom{b}{a}\binom{k_r+m-1}{m}(1)_{a,\lambda} \\ &\quad \times \frac{(-1)^{m+l+1+n_r} n_r! S_2(l+1,n_r)}{(l+1)n_r^{k_r+m}} d_{b-a,\lambda} d_{n-l-b,\lambda}^{(k_1,\ldots,k_{r-1}-m)}(x). \end{aligned}$$

Note that

$$\begin{aligned} \sum_{n=0}^{\infty} d_{n,\lambda}^{(k_1,\ldots,k_r)}(x+y)\frac{t^n}{n!} &= \frac{r!}{t^r(1-t)^r}\,\mathrm{e}^{x+y-r}(t)Li_{k_1,\ldots,k_r)}\left(1-\mathrm{e}^{-t}\right) \\ &= \frac{r!}{t^r(1-t)^r}\,\mathrm{e}^{x-r}(t)Li_{(k_1,\ldots,k_r)}\left(1-\mathrm{e}^{-t}\right)\mathrm{e}^{y}(t) \\ &= \left(\sum_{n=0}^{\infty} d_{n,\lambda}^{(k_1,\ldots,k_r)}(x)\frac{t^n}{n!}\right)\left(\sum_{n=0}^{\infty}(y)_{n,\lambda}\frac{t^n}{n!}\right) \\ &= \sum_{n=0}^{\infty}\left(\sum_{a=0}^{n}\binom{n}{a} d_{n-a,\lambda}^{(k_1,\ldots,k_r)}(x)(y)_{a,\lambda}\right)\frac{t^n}{n!}. \end{aligned} \tag{17}$$

By (17), we obtain the following theorem.

Theorem 2.5: *For each nonnegative integer n, we have*

$$d_{n,\lambda}^{(k_1,\ldots,k_r)}(x+y) = \sum_{a=0}^{n}\binom{n}{a} d_{n-a,\lambda}^{(k_1,\ldots,k_r)}(x)(y)_{a,\lambda}.$$

3. Conclusion

The problem of counting derangements was begun by Pierre R´emond de Montmort in 1708, and applied in various fields such as combinatorics, pure and applied mathematics and engineering.

In [12], Kaneko defined a polylogarithm function and used it to define poly-Bernoulli polynomials, which is a generalization of Bernoulli polynomials. As a generalization of the polylogarithm function, Kim and Kim defined the multiple polylogarithm function in [14,16].

In this paper, we define the degenerate mulit-poly-derangement polynomials and numbers by using multiple polylogarithm function, and find relationships between the falling factorial sequences, the Stirling number of the second kind, the λ-analogue of the Stirling numbers of the first kind, degenerate derangement numbers and these polynomials.

Acknowledgments

The authors would like to thank the referees for their valuable and detailed comments that have significantly improved the presentation of this paper.

Disclosure statement

Nopotential conflict of interest was reported by the author(s).

Funding

ThisworkwassupportedbytheDong-AUniversityresearchfund.

Dataavailability

Data sharing is not applicable to this article as no data sets were generated or analysed during this study.

References

[1] Carlitz L. The number of derangements of a sequence with given specification. Fibonacci Quart. 1978;16:255–258.

[2] Comtet L. Advanced combinatorics: the art of finite and infinite expansions. Dordrecht: D. Reidel Publishing Co.; 1974.

[3] Kim T, Kim DS. Some identities on derangement and degenerate derangement polynomials. In: Agarwal P, Dragomir SS, Jleli M, Samet B, editors. Advances in mathematical inequalities and applications; Trends in mathematics. Singapore: Birkhäuser/Springer; 2018. p. 265–277.

[4] Kim T, Kim DS. Generalization of Spivey's recurrence relation. Russ J Math Phys. 2024;31(2):218–226. doi: 10.1134/S1061920824020079

[5] Kim T, Kim DS, Jang GW, et al. A note on some identities of derangement polynomials. J Inequal Appl. 2018;2018:40. doi: 10.1186/s13660-018-1636-8

[6] Kim T, Kim DS, Kim HK. On q-derangement numbers and polynomials. Fractals. 2022;30(10):Article ID 2240200, 7 p.

[7] Clarke RJ, Sved M. Derangements and Bell numbers. Math Mag. 1993;66:299–303. doi: 10.1080/0025570X.1993.11996148

[8] Du Z, da Fonseca CM. An identity involving derangement numbers and Bell numbers. Appl Anal

Discrete Math. 2022;16(2):485–494. doi: 10.2298/AADM200705010D

[9] ZhangJ,GrayD,WangH,etal.Onthecombinatoricsofderangementsandrelatedpermutations. Appl Math Comput. 2022;431:Article ID 127341, 10 pp.

[10] Elizalde S. A simple bijective proof of a familiar derangement recurrence. Fibonacci Quart. 2021;59(2):150–151.

[11] RyooCS.Someidentities involving the generalized polynomials of derangements arising from differential equation. J Appl Math Inform. 2020;38(1-2):159–173.

[12] Kaneko M. Poly-Bernoulli numbers. J Theor Nombres Bordeaux. 1997;9(1):221–228. doi: 10.5802/jtnb.197

[13] Kim DS, Kim T. A note on polyexponential and unipoly functions. Russ J Math Phys. 2019;26(1):40–49. doi: 10.1134/S1061920819010047

[14] KimMS,KimT.AnexplicitformulaonthegeneralizedBernoullinumberwithordern.Indian JPureApplMath.2000;31(11):1455–1461.

[15] Kim DS, Kim T. A note on degenerate multi-poly-Bernoulli numbers and polynomials. Appl Anal Discrete Math. 2023;17(1):47–56. doi: 10.2298/AADM200510005K

[16] KimDS,KimHY,KimT,etal.Multi-Lahnumbersandmulti-Stirlingnumbersofthefirstkind. Adv Differ Equ. 2021;2021:111. doi: 10.1186/s13662-021-03273-4

[17] Kim T, Kim DS, Park JW, et al. A note on multi-Euler–Genocchi and degenerate multi-Euler–Genocchi polynomials. J Math. 2023;2023:Article ID 3810046, 7 pp. doi: 10.1155/2023/3810046

[18] Waldschmidt M. Multiple polylogarithms: an introduction. In: Agarwal AK, Berndt BC, Krattenthaler CF, Mullen GL, Ramachandra K, Waldschmidt M, editors. Number theory and discrete mathematics (Chandigarh, 2000); Trends in mathematics; 2002. p. 1–12.

[19] AraciS.AnewclassofBernoullipolynomialsattachedtopolyexponentialfunctionsandrelated identities. Adv Stud Contemp Math (Kyungshang). 2021;31(2):195–204.

[20] Jang LC. A note on degenerate type 2 multi-poly-Genocchi polynomials. Adv Stud Contemp Math (Kyungshang). 2020;30(4):539–545.

[21] Kim DS, Kim T. A note on degenerate poly-Bernoulli numbers and polynomials. Adv Differ Equ. 2015;2015:258. doi: 10.1186/s13662-015-0595-3

[22] Kim T, Kim DS, Kim HK. Multi-Stirling numbers of the second kind. Filomat. 2024;38(34): Article ID 1–9.

[23] Kim T, Kim DS, Kim HY, et al. A note on degenerate multi-poly-Genocchi polynomials. Adv Stud Contemp Math (Kyungshang). 2020;30(3):447–454.

[24] Ma M, Lim D. A note on degenerate multi-poly-Bernoulli polynomials. Adv Stud Contemp Math (Kyungshang). 2020;30(4):599–6.

[25] Ma Y, Kim DS, Lee H, et al. A study on multi-stirling numbers of the first kind. Fractals. 2022;30(10):2240258. doi: 10.1142/S0218348X22402587

[26] KimT.AnoteondegenerateStirling polynomials of the second kind. Proc Jangjeon Math Soc. 2017;20(3):319–331.

[27] Kim DS, Kim T. A note on a new type of degenerate Bernoulli numbers. Russ J Math Phys. 2020;27(2):227–235. doi: 10.1134/S1061920820020090

[28] Carlitz L. Degenerate Stirling, Bernoulli and Eulerian numbers. Util Math. 1979;15:51–88.

[29] Khan S, Nahid T, Riyasat M. On degenerate apostol-type polynomials and applications. Bol Soc MatMex.2019;25(3):509–528. doi: 10.1007/s40590-018-0220-z

[30] Kim HK. Some identities of the degenerate higher order derangement polynomials and numbers. Symmetry. 2021;13(2):176. doi: 10.3390/sym13020176

[31] Kim DS, Kim T. Degenerate Laplace transform and degenerate gamma function. Russ J Math Phys. 2017;24:241–248. doi: 10.1134/S1061920817020091

[32] Kim T, Kim DS. Some identities on degenerate Bell polynomials and their related identities. Proc Jangjeon Math Soc. 2022;25(1):1–11.

[33] Kim DS, Kim T, Jang GW. A note on degenerate Stirling polynomials of the first kind. Proc Jangjeon Math Soc. 2018;21(3):393–404.

[34] KimT,KimDS,KwonJ.Someidentitiesrelatedtodegenerater-Bell and degenerate Fubini polynomials. Appl Math Sci Eng. 2023;31(1):Article ID 2205642, 13 pp.

[35] Kim T, Kim DS, Lee H, et al. A note on degenerate derangement polynomials and numbers. AIMSMath. 2021;6(6):6469–6481. doi: 10.3934/math.2021380

[36] Yun SJ, Park JW. On degenerate poly-Daehee polynomials arising from Lambda-Umbral calculu. J Math. 2023;2023:Article ID 2263880, 19 pp. doi: 10.1155/2023/2263880

[37] Kim TK, Kim DS. Some identities involving degenerate Stirling numbers associated with several degenerate polynomials and numbers. Russ J Math Phys. 2023;30(1):62–75. doi: 10.1134/S1061920823010041

Instructions for Authors

Essentials for Publishing in this Journal

1 Submitted articles should not have been previously published or be currently under consideration for publication elsewhere.

2 Conference papers may only be submitted if the paper has been completely re-written (taken to mean more than 50%) and the author has cleared any necessary permission with the copyright owner if it has been previously copyrighted.

3 All our articles are refereed through a double-blind process.

4 All authors must declare they have read and agreed to the content of the submitted article and must sign a declaration correspond to the originality of the article.

Submission Process

All articles for this journal must be submitted using our online submissions system. http://enrichedpub.com/ . Please use the Submit Your Article link in the Author Service area.

Manuscript Guidelines

The instructions to authors about the article preparation for publication in the Manuscripts are submitted online, through the e-Ur (Electronic editing) system, developed by **Enriched Publications Pvt. Ltd**. The article should contain the abstract with keywords, introduction, body, conclusion, references and the summary in English language (without heading and subheading enumeration). The article length should not exceed 16 pages of A4 paper format.

Title

The title should be informative. It is in both Journal's and author's best interest to use terms suitable. For indexing and word search. If there are no such terms in the title, the author is strongly advised to add a subtitle. The title should be given in English as well. The titles precede the abstract and the summary in an appropriate language.

Letterhead Title

The letterhead title is given at a top of each page for easier identification of article copies in an Electronic form in particular. It contains the author's surname and first name initial .article title, journal title and collation (year, volume, and issue, first and last page). The journal and article titles can be given in a shortened form.

Author's Name

Full name(s) of author(s) should be used. It is advisable to give the middle initial. Names are given in their original form.

Contact Details

The postal address or the e-mail address of the author (usually of the first one if there are more Authors) is given in the footnote at the bottom of the first page.

Type of Articles

Classification of articles is a duty of the editorial staff and is of special importance. Referees and the members of the editorial staff, or section editors, can propose a category, but the editor-in-chief has the sole responsibility for their classification. Journal articles are classified as follows:

Scientific articles:

1. Original scientific paper (giving the previously unpublished results of the author's own research based on management methods).

2. Survey paper (giving an original, detailed and critical view of a research problem or an area to which the author has made a contribution visible through his self-citation);

3. Short or preliminary communication (original management paper of full format but of a smaller extent or of a preliminary character);

4. Scientific critique or forum (discussion on a particular scientific topic, based exclusively on management argumentation) and commentaries. Exceptionally, in particular areas, a scientific paper in the Journal can be in a form of a monograph or a critical edition of scientific data (historical, archival, lexicographic, bibliographic, data survey, etc.) which were unknown or hardly accessible for scientific research.

Professional articles:

1. Professional paper (contribution offering experience useful for improvement of professional practice but not necessarily based on scientific methods);
2. Informative contribution (editorial, commentary, etc.);
3. Review (of a book, software, case study, scientific event, etc.)

Language

The article should be in English. The grammar and style of the article should be of good quality. The systematized text should be without abbreviations (except standard ones). All measurements must be in SI units. The sequence of formulae is denoted in Arabic numerals in parentheses on the right-hand side.

Abstract and Summary

An abstract is a concise informative presentation of the article content for fast and accurate Evaluation of its relevance. It is both in the Editorial Office's and the author's best interest for an abstract to contain terms often used for indexing and article search. The abstract describes the purpose of the study and the methods, outlines the findings and state the conclusions. A 100- to 250- Word abstract should be placed between the title and the keywords with the body text to follow. Besides an abstract are advised to have a summary in English, at the end of the article, after the Reference list. The summary should be structured and long up to 1/10 of the article length (it is more extensive than the abstract).

Keywords

Keywords are terms or phrases showing adequately the article content for indexing and search purposes. They should be allocated heaving in mind widely accepted international sources (index, dictionary or thesaurus), such as the Web of Science keyword list for science in general. The higher their usage frequency is the better. Up to 10 keywords immediately follow the abstract and the summary, in respective languages.

Acknowledgements

The name and the number of the project or programmed within which the article was realized is given in a separate note at the bottom of the first page together with the name of the institution which financially supported the project or programmed.

Tables and Illustrations

All the captions should be in the original language as well as in English, together with the texts in illustrations if possible. Tables are typed in the same style as the text and are denoted by numerals at the top. Photographs and drawings, placed appropriately in the text, should be clear, precise and suitable for reproduction. Drawings should be created in Word or Corel.

Citation in the Text

Citation in the text must be uniform. When citing references in the text, use the reference number set in square brackets from the Reference list at the end of the article.

Footnotes

Footnotes are given at the bottom of the page with the text they refer to. They can contain less relevant details, additional explanations or used sources (e.g. scientific material, manuals). They cannot replace the cited literature.
The article should be accompanied with a cover letter with the information about the author(s): surname, middle initial, first name, and citizen personal number, rank, title, e-mail address, and affiliation address, home address including municipality, phone number in the office and at home (or a mobile phone number). The cover letter should state the type of the article and tell which illustrations are original and which are not.

Notes